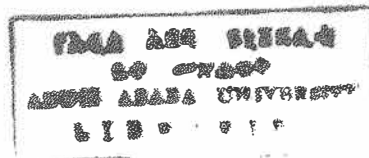


ELECTRIC AND MAGNETIC PROPERTIES OF HIGH- T_c OXIDE SUPERCONDUCTORS

A Thesis presented to the School of
Graduate Studies
Addis Ababa University

In partial fulfillment of the requirements
for the Degree Master of Science in Physics



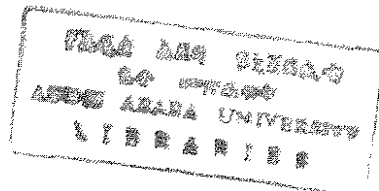
by
SAMUEL HAILU

OCT/1993

ACKNOWLEDGEMENT

My first and foremost heartfelt gratitude to my advisor and instructor Dr. I.M. Kashirsky. I would also like to thank Dr. G.X. Tessema (Climson University, USA) who provide us with samples and silver paste.

I would like to take this opportunity to record their sincere thanks for all those who have either directly or indirectly helped in the completion of my work.



ABSTRACT

The theories of conventional super conductivity are reviewed. We have investigated the electric and magnetic properties using different experimental techniques such as seebeck effect measurement, Hall effect measurement, and standard four - probe method.

Based on the experiment, transition temperature and carrier concentration are estimated. Our samples behave metallic above transition temperature. To explain the superconducting mechanism, exciton mechanism is discussed with respect to ABB (Allender, Bray and Bardeen) model:- a thin metallic layer on a semiconductor surface. Using computer simulation, we observe that our results agree with theoretical proposed exciton mechanism model (ABB).

INTRODUCTION	1
------------------------	---

CHAPTER -1-

FUNDAMENTAL PROPERTIES OF CONVENTIONAL SUPERCONDUCTORS	5
1.1 Discovery of Superconductivity	5
1.2 Physical properties of superconductivity	7
1.2.1 Persistent current	7
1.2.2 The Critical Magnetic Field	8
1.2.3 Meissner - Ochenfeld Effect of Flux Exclusion	9
1.2.4 Londons' Electromagnetic Equations	10
1.2.5 The Pippard Nonlocal Electrodynamics . .	13
1.3 Intermediate state (Vortex state)	16
1.4 Ginsburg - Landau theory	18
1.5 Thermodynamic properties of Superconductors . .	20

CHAPTER - 2 -

THE MICROSCOPIC THEORY OF SUPERCONDUCTIVITY

(BCS Theory)	24
2.1 Electron - Electron Interaction	24
2.2 Cooper Pair	25
2.3 Origin of The Attraction Interaction Between Electrons	30
2.4. Isotope Effect	32
2.5 Superconducting energy gap	33
2.6 Josephson Effect	36

CHAPTER III

HIGH - Tc OXIDE SUPERCONDUCTORS	40
3.1 The search for high - Tc superconductivity . .	40
3.2 Structure of high - Tc oxides	40

3.2	Structure of high - T _c oxides	40
3.3	Charge - transfer model	43
3.4	Physical Properties of Perovskite Oxides	43
3.5	The Superconducting States in High - T _c Superconductors	44
3.6	Superconducting Gap	46
3.7	High - T _c Oxide Superconductor without a Rare - Earth Element	46
3.8	Isotope Effect in the high - T _c Superconductors	48
3.9	Exciton Mechanism of superconductivity	50

CHAPTER IV

EXPERIMENTAL STUDY ON 123, 2212 AND 2223 PHASES OF OXIDE SUPERCONDUCTORS		63
4.1	Sample Preparation	63
4.1.1	1-2-3 Compound (Y ₁ Ba ₂ Cu ₃ O ₇)	63
4.1.2	2-2-1-2 Phase (Bi ₂ Sr ₂ CaCu ₂ O _x)	63
4.1.3	2-2-2-3 phase [(Bi,Pb) ₂ Sr ₂ Ca ₂ Cu ₃ O _x]	63
4.2	Structure Investigation	64
4.3	Investgation of Resistance Dependence on Temperature	68
4.4	Hall Effect Measurement	72
4.5	Thermopower (Seebeck Effect) Measurement	75
4.6	Meissner Effect on High - T _c Oxides	78
4.7	Investigation of the Transition Temperature	85
CHAPTER 5	CONCLUSIONS	92
	APPENDIX	94
	REFERENCE.	98

INTRODUCTION

The history of superconductivity starts back in 1911, when Kammerlingh Onnes [1] and one of his assistants discovered that the phenomenon of superconductivity while studying the resistivity of metal at low temperatures. Much to their surprise the resistance of the mercury sample dropped sharply at 4.5 k to an immeasurable small value. The immediate question that arose concerning the disappearance of resistance below the transition temperature (T_c) was whether it is zero or just too small to be measured with the accuracy of the available measuring instruments. To verify this, a ring of lead above its transition temperature was placed in a magnetic field and cooled below T_c . Upon removing the field, it has been observed that the current persists as long as the experimenter is disposed to wait, say in years. Such experiments allow a lower limit for the resistance of the superconductor, to all intents and purposes, zero.

The second extraordinary property of superconductors is that when a magnetic field is applied on a superconductor below its transition temperature, no magnetic field penetrates the specimen or it is possible to say that superconductors behave as a perfect diamagnetic.

These two extraordinary properties of superconductors, the disappearance of resistance and perfect diamagnetism, are explained by London's electromagnetic equation [2].

If a superconductor is placed in a strong magnetic field, superconductivity will disappear and it will reappear when the field is removed. In response to the field, superconductors are classified as type I and type II.

BCS theory (Bardeen, Cooper and Schrieffer)[2] succeeded in explaining the microscopic mechanism of superconductors. The central feature of this mechanism involves the electron-electron interaction via phonon media, and these interacting electrons form a bound state called cooper pair, with equal and opposite momentum and spin.

Superconductivity occurs when the electron-electron attraction interaction via phonons dominate the usual coulomb repulsive interaction.

Some of the applications of superconductors are low - loss electrical power transmission, magnetic levitation, weak magnetic field measurements, high magnetic field production for nuclear fusion reactor, electronic devices etc.

Shortcoming of conventional (low temperature) superconductors is that they are characterized with few kelvin transition temperature. To put such materials into applications, it is necessary to use Helium gas which is expensive to produce and costly to liquify.

To discover new materials with higher superconducting transition temperature has been one of the outstanding problems in solid-state physics ever since the discovery of superconductivity in 1911.

In 1986 a new class of high - T_c superconductors was discovered by Alex muller and George Bednortz. These new materials are multiphased oxides, of Lanthanum, Barium and Copper (La-Ba-Cu-O) With transition temperature up to 40k and with a span of few months, Yttrium substitution leads to transition temperature above 90k in Y-Ba-Cu-o. such material have perovskite structure and are called ceramics [3].

Although the scientific understanding of superconductors has attained remarkably great advancement there is still no satisfactory explanation of the superconducting conduction mechanism in High-Tc superconductors. So far the superconducting mechanism leading to high - Tc superconductors remains elusive.

The investigated samples are $Y_1Ba_2Cu_3O_7$ (123 phase), $(Bi,Pb)_2 Sr_2 Ca_2Cu_3O_{10}$ (2223 phase) and $Bi_2Sr_2Ca_1Cu_2O_8$ (2212 phase)

The main objective of our work is the application of ABB model, based on the exciton mechanism to explain the superconducting mechanism in 123,2223 and 2212 phase. The exciton mechanism is discussed with respect to ABB model. - a thin metallic layer on a semiconductor surface. Since high-Tc oxide superconductors are sandwich structures with alternating layers of metal-semiconductor metal, this model works quite well.

This thesis is organized as follows:

Chapter I, contains the discovery and physical properties of conventional superconductors. This can serve as a background for the study of high -Tc superconductivity.

Chapter II, is devoted to the description of microscopic superconducting mechanism of conventional superconductivity, i.e, BCS theory.

Chapter III. is discussion of processing, structure and physical properties of high - Tc oxides.

In chapter IV, we present the experimental results with necessary theoretical background. The experiments are resistance measurement as a function of temperature, Hall effect measurement, X-ray spectroscopy, thermopower

measurement, investigation of the transition temperature and observation of meissner effect.

In chapter V, conclusion of the experimental work will be presented. Computer simulation programs and references will be given at the end.

CHAPTER -1-

FUNDAMENTAL PROPERTIES OF CONVENTIONAL SUPERCONDUCTORS

1.1 Discovery of Superconductivity

The behavior of electrical resistivity was among the first problems investigated by Kammerlingh Onnes after he had achieved the liquefaction of Helium [1]. In 1911, measuring the resistance of mercury sample as a function of temperature, he had found that at about 4K the resistance falls abruptly to a value which Onnes best effort could not distinguish from Zero. This extraordinary phenomenon He called Superconductivity and the temperature at which it appears the critical temperature, T_c . [1]

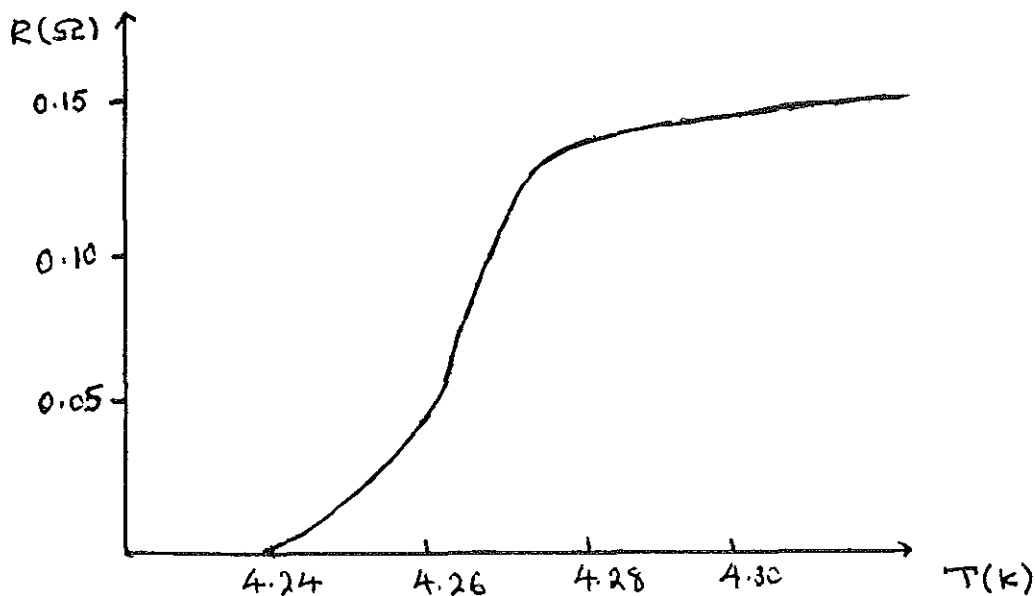


Fig 1.1 Resistance of Hg Vs temperature
(after Kamerling ones) [2]

As regards the scope of superconductivity, it has been found that some of the metallic elements are known to be superconductors in their normal forms, and other became superconducting under pressure or when prepared in the form of

disordered thin films . The number of known superconducting compounds and alloys run into thousands. Superconducting is thus a rather common characteristics of metallic conductors , so much so that its absence is often more unusual and striking than its presence. [3]

No, particular type of crystal lattice seems to be superconducting , since nearly all the types are represented in the list of known superconductors . By this, we do not of course, mean to imply that the crystal lattice is of less importance than the atomic species of the metal, for just as with ordinary conductivity, any change of crystal lattice for a metal of a given atomic species can have a profound effect.

Table 1 Transition temperature of some conventional superconductors [4]

Compound or element	T _c (k)
Al	1.19
Zn	0.815
Pb	7.18
Sn	3.72
Nb ₃ Sn	18.05
Nb ₃ Al	17.5
V ₃ Ga	16.5
V ₃ Si	17.1
Ti ₂ Co	3.44
La ₃ In	10.4

1.2 Physical properties of superconductivity

1.2.1 Persistent current

The remarkably high electrical conductivity was shown most

dramatically by observing an electrical current induced in a ring. A ring of lead was placed in a magnetic field above the transition temperature, and then cooled below the transition temperature. When magnetic field was removed, and it was found that the current induced in the metal persisted for as long as a time as the experiment was disposed to wait.

The constancy of the current in a superconducting ring offers the most accurate confirmation for the effectively zero resistance of the metal in the superconducting state. If in fact there was any electromotive force associated with the current, energy would be lost in the form of joul heat, and the current would die away in accordance with the relation [5]

$$L \frac{dI}{dt} + RI = 0 \quad (1.1)$$

Integrating,

$$I(t) = I_0 e^{-Rt/L} \quad (1.2)$$

where , R - resistance of the ring
 L - inductance of the ring
 I - current
 t - time

The time decay of the current , $\tau = L/R$, for a metal at low temperature but not superconductor is, for any practical dimensions of the ring, fairly short, usually not more than a few seconds; for a superconductor, however, even with a ring of very tin wire or a thin film coated on a non-superconductivity wire (to increase the hypothetical R), no decay of the current could be observed over several hours.

1.2.2 The Critical Magnetic Field

When a superconducting material is placed in sufficiently strong magnetic field, the superconductivity can be destroyed. However, it reappears when the field is removed. This minimum magnetic field required to destroy the superconducting at a given temperature depends on the shape and orientation of the specimen. If the specimen is in the shape of a long cylinder and is placed parallel to the field, the transition is sharp and the minimum field required to destroy the superconductivity is called the Critical field (H_c) [6].

The temperature dependence of H_c for most superconductors is well represented by [2]

$$H_c(T)/H_c(0) = 1 - (T/T_c)^2 \quad (1.3)$$

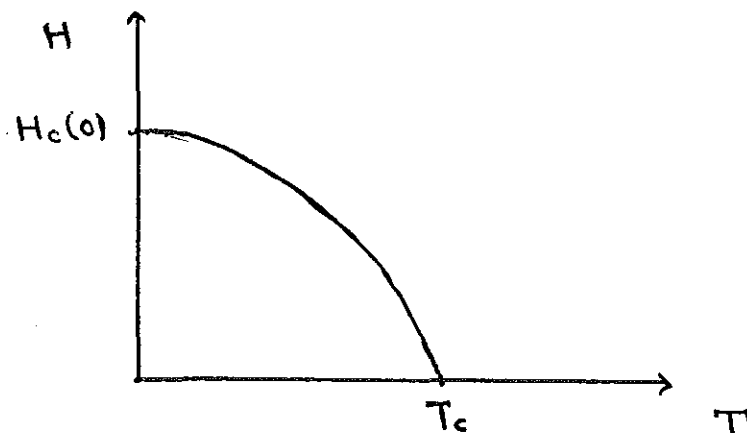
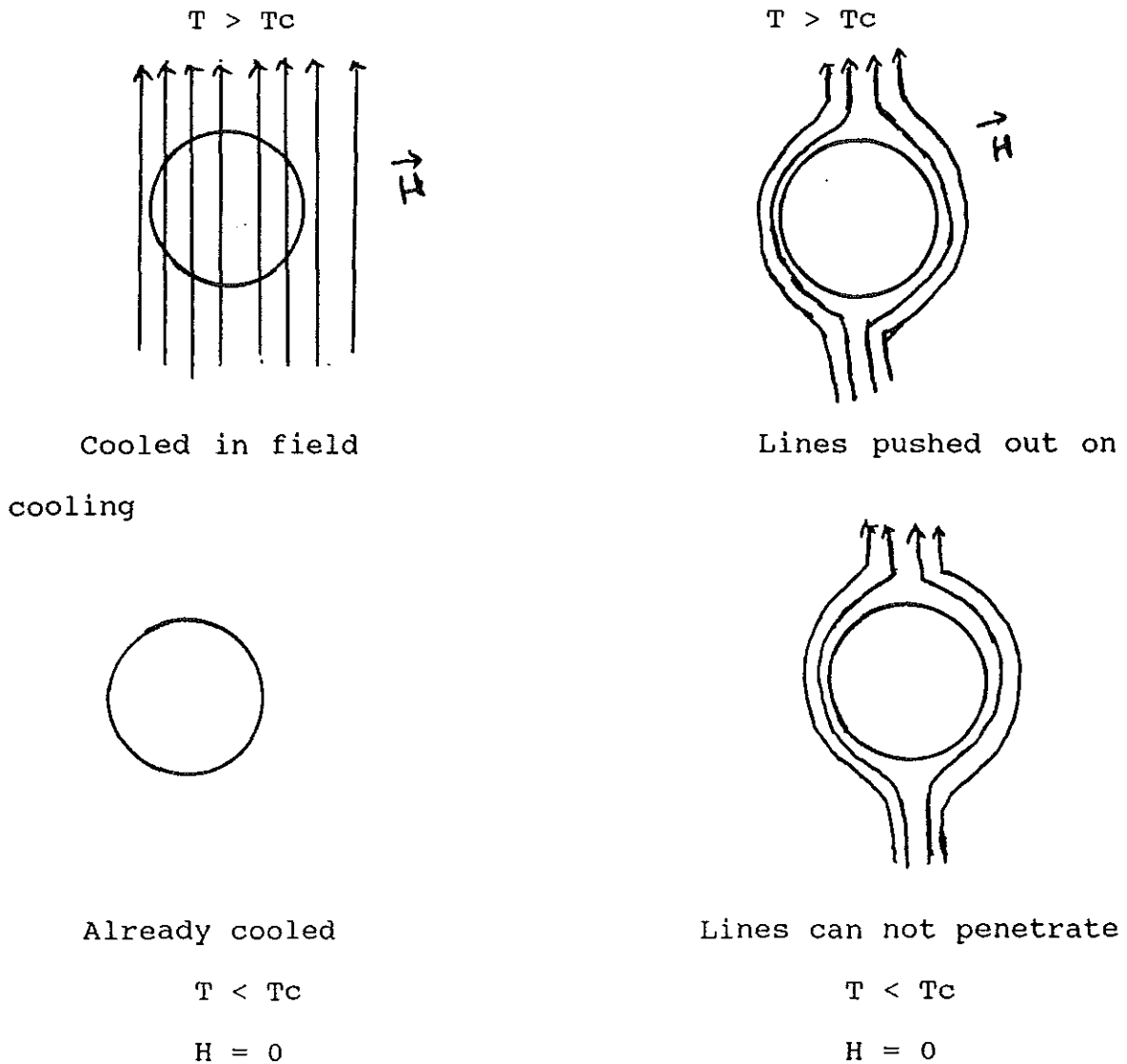


Fig 1.2 Temperature dependance of the critical field.

1.2.3 Meissner - Oshenfeld Effect of Flux Exclusion

In 1933 Meissner and Oshenfeld showed that if a long cylindrical superconductor is cooled in a longtiudnal magnetic field below its transition temperature T_c , the lines of

induction will be pushed out of the material due to infinite conductivity.



On the other hand if the material is cooled initially below transition temperature and then placed in a magnetic field, a flux will not penetrate the material. [6]

Meissner effect shows that a superconductor behaves as if inside the specimen we have zero magnetic field ($B = 0$)

Hence from, [6]

$$\vec{B} = \vec{H} + 4\pi\vec{M} \quad (1.4)$$

where

\vec{B} = Magnetic induction

\vec{H} = Magnetic field

\vec{M} = Magnetization

For $B = 0$, we have

$$\vec{H} = -4\pi\vec{M}$$

but

$$\vec{M} = X\vec{H} \quad (1.5)$$

where X is magnetic susceptibility

Thus

$$X = -1/4\pi$$

(1.6)

A superconductor exhibits a perfect diamagnetization. This suggests that perfect diamagnetization and zero resistance are two independent properties of superconducting states.

1.2.4 Londons' Electromagnetic Equations

To account for the electromagnetic properties of superconductors, in particular to account for Meissner effect and the existence of persistent currents, F. and H. London proposed that ohm's law, which relates current density by other relations connecting the superconducting currents and fields in superconductors. The relations are [2]

$$\vec{E} = \partial/\partial t (\lambda \vec{J}_s) \quad (1.7)$$

$$\vec{H} = -C \text{curl} (\lambda \vec{J}_s) \quad (1.8)$$

Where \vec{H} and \vec{E} are Magnetic and Electric fields

\vec{J}_s is current density

$\lambda = 4\pi\lambda_L^2/c^2 = m/n_s e^2$, is a phenomenological (1.9)
parameter

λ_L = Penetration depth

n_s = Number density of superconducting electrons

m = electron mass

c = speed of light.

The total current density \vec{J} consists of normal currents \vec{J}_n and supercurrent \vec{J}_s , such that [6]

$$\vec{J} = \vec{J}_n + \vec{J}_s \quad (1.10)$$

for $T = T_c$, $\vec{J} = \vec{J}_s$ (1.11)

Further more since superconducting electrons move freely without resistance so an electron field \vec{E} can only give the electrons an acceleration a , then

$$e\vec{E} = m d\vec{v}/dt \quad (1.12)$$

If n is the number of superconducting electrons per unit volume and \vec{v} their average velocity then the current density \vec{J} is given by

$$\vec{J} = ne\vec{v} \quad (1.13)$$

and $d\vec{J}/dt = ned\vec{v}/dt$ (1.14)

From equation (1.12) and (1.14), we have

$$d\vec{J}/dt = ne^2\vec{E}/m = \vec{E}/\lambda$$

or $\vec{E} = \lambda d\vec{J}_s/dt$ (1.15)

Taking the curl of both sides of equation (1.15)

But from Maxwell equation we know that (in Gaussian unit)

$$\text{curl } \vec{E} = \text{curl} (\lambda \partial \vec{J}_s / \partial t) \quad (1.16)$$

$$\text{curl } \vec{E} = -1/c \times \partial \vec{H} / \partial t \quad (1.17)$$

From this two equations we have,

$$\text{curl } \lambda \frac{\partial \vec{J}_s}{\partial t} = -\frac{1}{c} \times \frac{\partial \vec{H}}{\partial t} \quad (1.18)$$

Integrating equation (1.18) we get,

$$C \text{ curl } \lambda \vec{J}_s = -\vec{H} \quad (1.19)$$

Equation (1.19) is the fundamental equation of the superconducting state, current J_s is maintained by local field H .

Londons' electromagnetic equation (1.17) combined with Maxwell equation (1.17), leads to

$$\vec{H} = -c^2/4\pi \text{ curl} (\text{curl } \vec{H})$$

Using the vector identity, $\text{curl curl } H = \text{grad div } H - \nabla^2 H$

$$\vec{H} = (-\lambda c^2/4\pi) \times [\text{grad div } \vec{H} - \nabla^2 \vec{H}]$$

but from Maxwell equations, $\text{div } H = 0$

Thus ;

$$\vec{H} = \frac{\lambda c^2}{4\pi} (\nabla^2 \vec{H}) \quad (1.20)$$

or

$$\nabla^2 \vec{H} = \lambda_L^2 \vec{H} \quad , \quad \text{where } \lambda_L^2 = \frac{\lambda c^2}{4\pi}$$

This implies that the magnetic field is exponentially screened from the interior of a sample with penetration depth λ_L , that is Meissner effect.

The solution of equation (1.20) is of the form

$$H(x) = H(0) \exp[-x/\lambda_L] \quad (1.21)$$

Where x is the distance inside the sample from the surface. For large values of x , the field is almost zero. (Meissner effect)

1.2.5 The Pippard Nonlocal Electrodynamics

Pippard introduced the coherence length while proposing a non local generalization of London equations [7]. He argued that the superconducting wave function should have a similar characteristic dimensions ξ_0 (coherence length) which could be estimated by the uncertainty principle, as follows; only electrons within KT_c of the Fermi energy can play a major role in a phenomenon which sets in at T_c , and these electrons have a momentum range, Δp [7].

$$\Delta p = \frac{KT_c}{V_f} ,$$

Where V_f is the Fermi velocity

From the uncertainty principle

$$\Delta x \cdot \Delta p \geq \hbar$$

substituting for p

$$\Delta x \geq \frac{\hbar}{\Delta p} \approx \hbar \frac{V_f}{KT_c}$$

Leading to the definition of coherence length

$$\xi_0 = \hbar V_F / K T_C \quad (1.22)$$

Londons' equation applies when \vec{J} and \vec{A} vary slowly in space on the scale ξ_0 (coherence length). In general, we may guess that the current $\vec{J}(r)$ at one point will depend on the vector potential $A(r')$ at all neighboring point r' such that

$$|\vec{r} - \vec{r}'| < \xi_0$$

A phenomenological relation constructed to describe this effect, has been proposed by Pippard as [8]

$$\vec{J}(r) = 3/4\pi\lambda c\xi_0 \int \left(\frac{(\vec{A}(r') \cdot \vec{R}) \vec{R} \exp(-R/\xi_0)}{R^4} \right) dr' \quad (1.23)$$

where c is speed of light

$$\begin{aligned} \vec{R} &= \vec{r} - \vec{r}' \\ \lambda &= m/n e^2 \end{aligned}$$

The penetration depth λ can be estimated by intuitive argument of Pippard's : If A was essentially constant on a thickness ϵ_0 near the surface, we would have, in this region from Pippard equation

$$\vec{J} = \left(\frac{-ne^2}{mc} \right) \vec{A} \quad (\text{London result})$$

But infact A is non zero only in a smaller thickness λ . Thus the integral equation (1.23) is reduced, roughly by the factor λ/ξ_0 .

where λ is defined self - consistently by

Thus,

$$\vec{J} = \left(\frac{-ne^2}{mc} \right) \left(\frac{\lambda}{\xi_0} \right) \vec{A} \quad \text{for } (\lambda \ll \xi_0) \quad (1.24)$$

$$\frac{1}{\lambda^2} = \left(\frac{4\pi ne^2}{mc^2} \right) \frac{\lambda}{\xi_0}$$

$$\lambda^3 = \lambda_I^2 \xi_0 \quad \text{for } (\lambda \ll \xi_0)$$

A (much more complicated) rigorous calculation gives.

$$\lambda = \left[\left(\frac{\sqrt{3}}{2\pi} \right) \xi_0 \lambda_I^2 \right]^{1/3}$$

Table 2. characteristic lengths of some superconductors [7]

Element	λ_L (Å)	ϵ_0 (Å)	λ_{th} (Å)	λ_{exp} (Å)
Al	157	16,000	530	490 - 515
Sn	355	2,300	560	510
Pb	370	830	460	390

1.3 Intermediate state (Vortex state)

In deriving the London equation, one may assume a slow variation in space of the velocity $\vec{V}(r)$ or of the super-current $J_s(r)$. By "slow" we mean, in the condensed state, the velocity of the two electrons e_1 and e_2 are correlated if the distance between them R_{12} is smaller than a certain range, i.e. correlation length ξ_0 . The derivation applies when $V(r)$ has a negligible variation over distance ξ_0 . [7]

In simple (non transition) metals λ_L is small ($= 300 \text{ \AA}$). The Fermi velocity V_F is large ($V_F \geq 10^8 \text{ cm/sec}$), and $\xi_0 = 10^4 \text{ \AA}$ for Al. Thus for these metals the London equation does not apply. Infact they do exhibit the Meissner effect, but in order to calculate the penetration depth it is necessary to replace the London equation by a some what more complicated relation,

the form which has been suggested by Pippard. We call these first kind (TYPE I) or Pippard superconductors [7].

For transition metals and intermetallic compound of the type Nb_3Sn , V_3Ga , the effective mass is very large, λ_L is large (200 Å) and the Fermi velocity is small ($= 10^6$ cm/sec). Also, in these compounds the transition temperature above which superconductivity disappears is found to be high (18°K in Nb_3Sn). For all these reasons ϵ_0 is very small (≈ 50 Å). Therefore for these class of materials London equation is well applicable in weak fields. We call this second kind (TYPE II) or London equations. Superconductors can be classified as TYPE I or TYPE II. in response to magnetic field.

TYPE I superconductors are characterized by a single critical magnetic field H_c , above which they are normal and below which they are superconductors (as in fig. (1.2)). But TYPE II are characterized by two critical fields, designed as H_{c1} and H_{c2} , when the applied field is less than the lower critical field H_{c1} , the material is entirely superconducting and there is no flux penetration, just as in the case of type I. When the applied field exceeds the upper critical field H_{c2} , the flux penetrates completely and the superconducting state is destroyed. However , for fields lying between H_{c1} and H_{c2} the material is in mixed state, often referred to as the vortex state or mixed state (Shubnikov phase) [7].

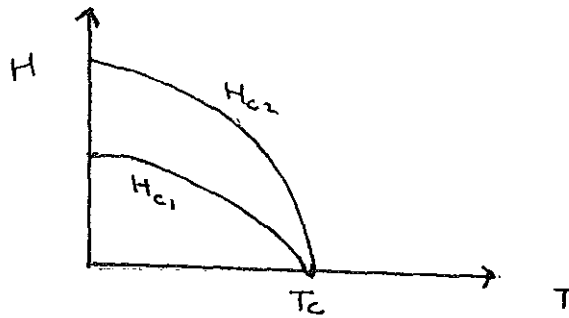


Fig 1.3 Temperature dependence of critical field for type II superconductors

While in the vortex, the material can have zero resistance and has partial flux penetration.

In the field interval H_{c1} to H_{c2} , the substance is said to be in the mixed state. A close examination of the substance of the specimen in this state reveals the presence of small circular regions in normal states, which are surrounded by a large superconducting region forming the remainder of the specimen. The small region are referred to as vortexes [Fig. 1.4].

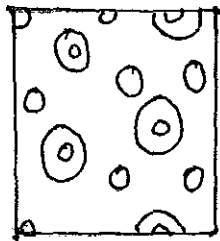


Fig 1.4 Vortex contour lines [7]

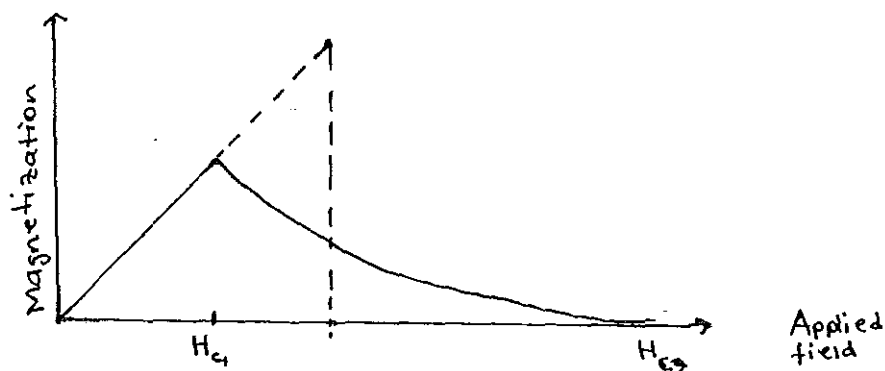


Fig 1.5 Magnetization curve as a function of applied magnetic field for type II [6]

1.4 Ginsburg - Landau theory

Superconducting state varies from something to nothing in the interface of type I superconductors, this theory describes a spatial variation of the superconducting state. That is, n_s , superconducting electrons must be a function of position. [8]

$$n_s = |\psi_s(x)|^2 \quad (1.25)$$

The strength of the superconducting can be described by Ψ . In normal state, Ψ is zero

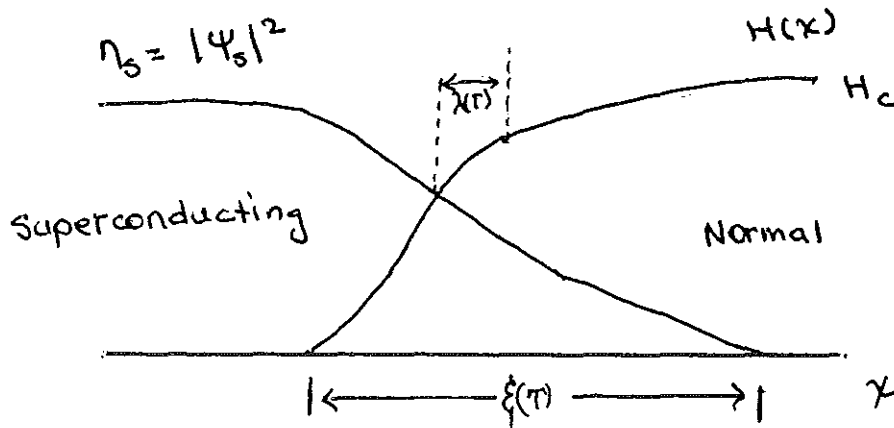


Fig 1.6 Interface between superconducting and normal domains in the intermediate state

Using a variational principle and working from an assumed expansion of the free energy in powers of Ψ and $\Delta\Psi$, they derived a differential equation. [9]

$$\frac{1}{2m^*} \left(\left(\frac{\hbar}{i} \right) \nabla - \left(\frac{e^*}{c} \right) A \right)^2 \psi + \beta |\Psi|^2 \psi = -\alpha(T) \psi \quad (1.26)$$

Which is very analogous to the Schrodinger equation for a free particle, but with a non linear term.

The corresponding equation for the super current

$$J_s = \frac{e^* \hbar}{i 2 m^*} (\psi^* \nabla \psi - \psi \nabla \psi^*) - \left(\frac{e^*}{m^* c} \right) |\psi|^2 A \quad (1.27)$$

With the G - L formalism it was able to treat two features which were beyond the scope of the London theory, namely [8]

- 1- Nonlinear effect in fields strong enough to change n_s (or $|\Psi|^2$)
- 2- Spatial variation of n_s

The G-L theory introduces a characteristic length, now called the temperature dependant coherence length

$$\xi(T) = \frac{\hbar}{2 m^* \alpha(T)^{1/2}} \quad (1.28)$$

In a pure superconductor for $T > T_c$

$$\xi(T) \approx \xi_0 \quad \text{Pippard coherence length}$$

near T_c , $\epsilon(T)$ diverges as $(T_c - T)^{-1/2}$

The ratio of the two lengths defines the G - L parameter

$$K = \frac{\lambda}{\xi} \quad (1.29)$$

Since λ and ϵ diverges in the same way as T_c this dimension less ratio is approximately independent of temperature.

1.5 Thermodynamic properties of Superconductors

The magnetic work stored per unit volume of material is given by

$$F_m = (4\pi)^{-1} \int_0^B H dB$$

If the Gibbs free energy of a specimen in the absence of magnetic field in superconducting state is G_n , then in an applied field H it is

$$\begin{aligned} G_s(H, T) &= G_s(0, T) - (4\pi)^{-1} \int_0^B H dB \\ &= G_s(0, T) - H^2/8\pi \end{aligned} \quad (1.30)$$

In the normal state the magnetic susceptibility is generally vanishingly small, thus

$$G_n(H) = G_n(0) \quad \text{Where } G_n \text{ is normal state Gibbs free energy.}$$

In equilibrium, at transition ($H = H_c$)

$$G_s(H_c) = G_n(H_c) = G_n(0)$$

Thus

$$\begin{aligned} G_s(0, T) - H_c^2/8\pi &= G_n \\ \text{or } G_s - G_n &= H_c^2/8\pi \quad \text{Condensation energy.} \end{aligned} \quad (1.31)$$

The entropy S , and specific heat per unit volume c , of the two state are given by

$$\begin{aligned} S_n &= -\frac{dG_n}{dT} & S_s &= -\frac{dG_s}{dT} \\ C_s &= T \frac{dS_s}{dT} & C_n &= T \frac{dS_n}{dT} \end{aligned} \quad (1.32)$$

The difference in entropy and specific heat can be expressed as, respectively,

$$\begin{aligned}
 S_n - S_s &= - \left(\frac{H_c}{4\pi} \right) \frac{dH_c}{dT} \\
 C_n - C_s &= - \left(\frac{T}{8\pi} \right) \frac{d^2 H_c^2}{dT^2}
 \end{aligned}
 \tag{1.33}$$

At $T = T_c$; $H_c = 0$

$$S_n = S_s$$

At any lower temperature

$$H_c > 0 \text{ and } dH_c/dT < 0 \quad \text{thus } S_n > S_s$$

Thus entropy of two phases are equal at the critical temperature in zero field. But at any lower temperature the entropy of superconductor is less than the normal one. Indicating that the superconducting state is the state of higher order. [2]

The latent heat of transition is

$$L = T (S_n - S_s) = - (T / 4\pi) H_c (dH_c/dT) \tag{1.34}$$

In the presence of magnetic field, the transition is of the first order. heat is evolved at the transition when the material is cooled from the normal to the superconductive state. This implies $dH_c/dT < 0$, i.e. Critical field decreases with increasing temperature.

For $H_c = 0$, $T = T_c$; the latent heat L vanishes under those conditions transition becomes " second order " and there is discontinuity in the specific heat at the transition temperature.

$$\begin{aligned}
 \Delta C_{T=T_c} &= C_s(T_c) - C_n(T_c) \\
 &= T_c/4\pi (dH_c/dT)^2_{T=T_c}
 \end{aligned}
 \tag{1.35}$$

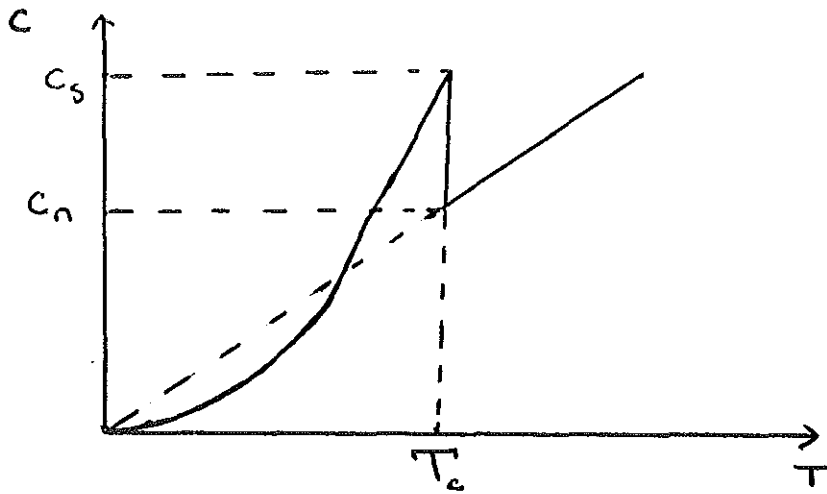


Fig 1.7 Variation of specific heat with temperature and its jump at T_c . [8]

$$H_c = H_0 [1 - (T/T_c)^2]$$

$$H_c^2 = H_0^2 [1 - (T/T_c)^2]$$

$$\begin{aligned} dH_c^2/dT &= -4H_0^2 [1 - (T/T_c)^2] T/T_c^2 \\ &= -4H_0^2/T_c^2 [1 - (T/T_c)^2] T \end{aligned}$$

$$d^2H_c^2/dT^2 = -4H_0^2/T_c^2 [1 - 3(T/T_c)^2]$$

But

$$\begin{aligned} C_s(T) - C_n(T) &= -T/8\pi d^2H_c^2/dT^2 \\ &= -T/8\pi \{ -4H_0^2 [1 - 3(T/T_c)^2] \} \end{aligned}$$

$$C_s(T) - C_n(T) = H_0^2/2\pi T_c^2 [T/T_c - 3(T/T_c)^3] \quad (1.36)$$

The first term should be the specific heat of the electrons in the normal state and if the lattice specific heat in the two states is assumed to be the same, then the second term must represent the specific heat of the electron in superconducting state. [2]

CHAPTER - 2 -

THE MICROSCOPIC THEORY OF SUPERCONDUCTIVITY

(BCS Theory)

2.1 Electron - Electron Interaction

BCS theory is the basis of a general quantum theory of conductivity given by Bardeen, Cooper and Schrieffer in 1957 [6]. They succeeded in showing that the basic interaction responsible for superconductivity appears to be that of a pair of electrons by means of an interchange of virtual phonons. At first it seems to encounter intuitive since electrons normally repel one another because of their like charges. However, a net attraction could be obtained if the electrons interact with each other via the motion of the crystal lattice as the lattice structure is momentarily deformed by passing electron.

This means that the lattice is distorted by a moving electron, this distortion giving rise to a phonon. A second electron some distances away is then affected when it is reached by the propagating fluctuation in the lattice charge

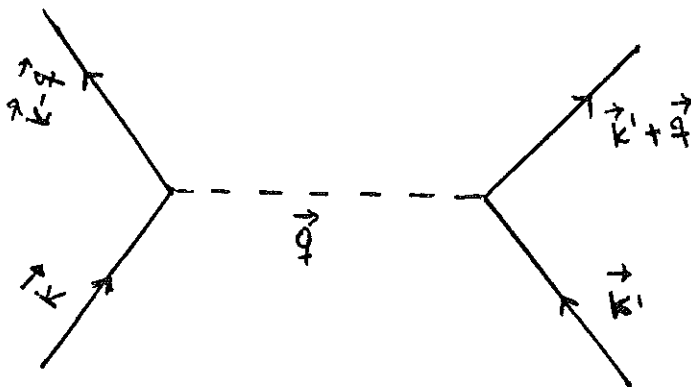


Fig 2.1 Electron - electron interaction via phonons

[10]

distribution. In other words, as shown in fig (2.1), an

electron of wave vector \vec{k} emits a virtual phonon \vec{q} , which is absorbed by an electron \vec{k}' . This scatters \vec{k} in to $\vec{k} - \vec{q}$ and \vec{k}' in to $\vec{k}' + \vec{q}$. The process being virtual one energy need not be conserved, and in fact the nature of resulting electron-electron interaction depends on the relative magnitudes of the electronic energy change and the phonon energy $\hbar\omega_q$. If this phonon energy exceeds electronic energy the interaction is attractive.

Thus superconductivity occurs when such an attractive interaction between two electrons, by means of phonon exchange, dominates the usual repulsive coulomb interaction.

2.2 Cooper Pair

Shortly before the formulation of the BCS theory, Cooper [6] had been able to show that if there is a net attraction, however weak, between a pair of electrons just above the Fermi surface, these electrons can form a bound state. The electrons for which this can occur as a result of the phonon interaction lie in a thin shell of width $\approx \hbar\omega_q$, where $\hbar\omega_q$ is of the order of the average phonon energy of the metal.

The two partners of a Cooper pair have opposite momenta and spin ($\vec{k}\downarrow$ and $-\vec{k}\uparrow$) [4]

Cooper pairs (zero spin) behave as bosons and can all be in the same state. This is in contrast to electrons which are fermions with spin $1/2$ that must obey the pouli-exclusion principle.

The BCS theory has been very successful in explaining the characteristic superconducting properties of zero resistance and flux expulsion. From a qualitative point of view, one can say that in order to reduce the momentum of a single pair by

scattering, it would be necessary to simultaneously reduce the momentum of all the other pairs. It is an "all or nothing at all situation".

Lattice imperfection and lattice vibrations which effectively scatter electrons in normal metals, have no effect on Cooper pairs. In the absence of scattering, the resistivity is zero.

To see how this binding comes about :

The ground state of a free electron gas corresponds to complete filling of the one - electron energy level of wave vector K and energy $\hbar^2 K^2/2m$ up to certain energy $E_F = \hbar^2 K_F^2/2m$ (the Fermi energy), However, in the presence of an attraction interaction, no matter how week , this state becomes unstable. This instability can be understood by considering two particular electrons of coordinates r_1 and r_2 , the other electrons still being treated as a free electron gas. The only effect of this electron gas is forbid the two electrons to occupy all states $K < K_F$ by exclusion principle. [7]

Let (r_1, r_2) be the wave function of the two electrons. Consider any state where the center of gravity of the pair (r_1, r_2) is at rest; is then only a function of $(r_1 - r_2)$. Expanding in plane waves

$$\psi(\vec{r}_1 - \vec{r}_2) = \sum_K g(\vec{K}) e^{i\vec{K}(\vec{r}_1 - \vec{r}_2)} \quad (2.1)$$

Where $g(K)$ is the probability amplitude for finding one electron in the plane wave state of momentum $\hbar K$ and other in the state $(-\hbar K)$

Since the state $K < K_F$ are already occupied, the Pauli exclusion principle imposes

$$g(\vec{K}) = 0 \quad \text{for } k < K_F \quad (2.2)$$

The Schrodinger equation for the two electron is

$$-\hbar^2/2m(\nabla_1^2 + \nabla_2^2) \psi(\vec{r}_1, \vec{r}_2) + V(\vec{r}_1, \vec{r}_2) \psi = (E + \hbar K_F/m) \psi \quad (2.3)$$

E is the energy of the pair relative to the state where the two electrons are at Fermi level.

On inserting equation (2.1) in to equation (2.3), we find an equation for $g(K)$,

$$\left(\frac{\hbar^2}{m}\right) K^2 g(\vec{K}) + \sum_{\vec{K}'} g(\vec{K}') V_{\vec{K}\vec{K}'} = (E + 2E_F) g(\vec{K}) \quad (2.4)$$

$$V_{\vec{K}\vec{K}'} = \left(\frac{1}{L^3}\right) \int V(\vec{r}) e^{i(\vec{K}-\vec{K}')\vec{r}} d\vec{r}$$

$V_{\vec{K}\vec{K}'}$ is the matrix element of the interaction between the electronic states \vec{K} and \vec{K}' , L^3 is the volume of the system.

Equation (2.4) together with the Pauli condition (2.2) is sometimes called the Bethe - Goldstone equation for the two - electron problem [7].

For $E > 2E_F$ it has a continuous spectrum describing the collisions of the two electrons from the initial state $(\vec{K}_1 - \vec{K})$ towards final state $(\vec{K}', -\vec{K}')$ of the same energy. But if the interaction V is attractive there may also be a bound state solutions with $E < 2E_F$. To see this, consider the simplified interaction.

$$\frac{\hbar^2 K^2}{2m} < E_F + \hbar \omega_D \quad (2.5)$$

$$V_{KK'} = -\frac{V}{L^3} \quad \text{for } \frac{\hbar^2 K^2}{2m} < E_F + \hbar \omega_D$$

$$= 0 \quad \text{other wise}$$

The interaction is attractive and constant in an energy band $\hbar \omega_D$ above the Fermi energy, then eqn (2.4) becomes

$$(\hbar^2 K^2/m + E + 2E_F) g(\vec{K}) = . c \quad (2.6)$$

Where C is independent of K

$$C = -\frac{V}{L^3} \sum_K g(\vec{K}')$$

$$E_F < \frac{\hbar^2 K^2}{2m} < E_F + \hbar \omega_D \quad (2.7)$$

Comparing eqn. (2.6) and (2.7), we find the self consistency condition

$$1 = \frac{V}{L^3} \sum_{K'} 1/((-E + \hbar^2 K^2/m) - 2E_F)$$

$$E_F < \frac{\hbar^2 K^2}{2m} < E_F + \hbar \omega_D \quad (2.8)$$

If we set

$$\xi' = \frac{\hbar^2 K^2}{2m} - E_F \quad (2.9)$$

and introduce the density of states per unit energy

The condition becomes

$$N(\xi') = (2\pi)^{-3} 4\pi K^2 \frac{dK'}{d\xi'}$$

$$1 = V \int_0^{\hbar\omega_D} N(\xi') \frac{1}{(2\xi' - E)} d\xi' \quad (2.10)$$

If we assume $\hbar\omega_D \ll E_F$, $N(\xi')$ can be considered as constant and replaced by its value $N(0)$ at the Fermi level; performing the integration.

$$1 = \frac{1}{2} N(0) V \ln \frac{E - 2\hbar\omega_D}{E} \quad (2.11)$$

and in the limit of weak interaction $N(0)V \ll 1$

$$E = -2\hbar\omega_D e^{-\frac{2}{N(0)V}} \quad (2.12)$$

Therefore there exists a two - electron bound state of energy $E < 0$.

If one start from a free electron gas, and turn on the interaction V , one predicts that the electrons will group themselves in pairs giving up energy to the external world. The normal state is thus unstable.

2.3 Origin of The Attraction Interaction Between Electrons

In a simple electron gas, the only interactions are Coulomb repulsion, and thus not favorable for the cooper phenomenon [8]. To obtain an attracting matrix element $V_{KK'}$, the electrons must be coupled to another system of particles, or excitations in solid.

There are many varieties of such excitations. We might try for that purpose -phonons, electrons from other bands, spin wave in magnetic media, and so on. Only one of the present, i.e the electron - phonon interaction.

Let's examine the origin of the negative $V_{KK'}$ needs for superconductivity.

If we take the bare Coulomb interaction $V(r) = e^2/r$ and carry out the computation of $V(q)$

$$V(\vec{q}) = V(\vec{K}-\vec{K}') = V_{KK'} = \Omega^{-1} \int V(\vec{r}) e^{i\vec{q}\cdot\vec{r}} dr \quad (2.13)$$

We find

$$V_{KK'} = V(\vec{q}) = \frac{4\pi e^2}{\Omega q^2} = \frac{4\pi e^2}{q} \quad (2.14)$$

since Ω :1 unit normalization

Now, If we take the dielectric functions $\epsilon(q, \omega)$ of the medium in to account, $V(q)$ is reduced by a factor $\epsilon^{-1}(q, \omega)$. The most obvious ingredient in $\epsilon(q, \omega)$ is the screening effect of the conduction electrons. [11] In the Fermi - Thomas approximation, ϵ is given by $\epsilon = 1 + K_s^2/q^2$.

$$\Rightarrow V = \frac{4\pi e^2}{q^2 + K_s^2} \quad (2.15)$$

Thus the electronic screening has limited the divergence at $q = 0$, but it still leaves a positive $V_{KK'}$. Hence no superconductivity would result. [7]

Negative terms comes only when one takes the motion of the ion cores in to account. The physical idea is that the first

electron polarizes the medium by attracting positive ions; these excess positive ions, in turn, attract the second electrons, giving an effective interaction between the electrons. If this attraction is strong enough to override the repulsive screened coulomb interaction, and superconductivity results.

It is clear that the characteristic vibrations, or phonones, frequency will play a role. For the electronically screened coulomb interaction, the characteristic frequency is the plasma frequency, which is so high that we assume instantaneous response.

From momentum conservation, we can see that if an electron is scattered from \vec{k} to \vec{k}' , the relevant phonon must carry the momentum $\vec{q} = \vec{k} - \vec{k}'$, and the characteristic frequency must then be the phonon frequency w_q . As a result, it is plausible that the phonon contribution to the screening function be proportional to $(w^2 - w_q^2)^{-1}$. Evidently this resonance denominator gives a negative sign if $w < w_q$, corresponding to the physical argument above, for higher frequencies, i.e. electron energy differences larger than $\hbar w_q$, the interaction becomes repulsive. Thus the cut off energy $\hbar w_c$ of cooper attractive matrix element $-V$ is expected to be the order of the Debye energy $\hbar w_D = K\theta_D$.

The first attempt to test the theoretical criteria for superconductivity systematically is by using the "Jellium" model, in which the solid is approximated by a fluid of electrons and point ions, with complete neglect of structure and Brillouin zone effect as well as the finite ion - core size.

Thus for the Jellium model

$$V(q, w) = 4\pi e^2 / (q^2 + K_s^2) + (4\pi e^2 / (q^2 + K_s^2)) (w_q^2 / (w^2 - w_q^2)) \quad (2.16)$$

where W is frequency of vibration

The first term is a screened Coulomb repulsion, and the second term is the phonon mediated interaction and is attractive for $w < w_q$

For an average phonon $w_q \approx w_D$ (Debye frequency of the material), thus the energy interval in which we find an attraction is of order of $\approx \hbar w_D = K_B \theta_D$. θ_D is typically of the order of 300 K and $K_B \theta_D$ is about 0.03 eV).

2.4. Isotope Effect

Maxwell and Serin [6] independently found that the critical temperature of superconductors varies with isotopic mass (as in equation 2.18). This indicates that superconductivity is due to an interactions between electrons and lattice vibrations. The experimental results are generally in agreement with the relation

$$M^{1/2} T_c = \text{Constant} \quad (2.17),$$

where M is mass for vibrations of a crystal with one atom, from dispersion relation we have [4]

$$W^2 \sim M^{-1} \quad (2.18)$$

Where W is frequency of vibration

M mass of the atom

2.5 Superconducting energy gap

One of the major stapes in understanding superconductors was the establishment of the existence of the energy gap between the ground state and the quasi - particle excitation of

the system. Such a gap has been suggested first by Dount and Mendelleson.

The main evidence of the energy gap comes from [8].

1- The low temperature behavior of the specific heat

$$\begin{aligned} C_{es} &\approx \gamma T_c a e^{\frac{-bT_c}{T}} \\ &\approx \exp\left(-\frac{\Delta}{KT}\right) \end{aligned} \quad (2.19)$$

Where a and b are constants

2Δ is the energy gap

C_{es} - electronic specific heat under constant volume

The normal - state electronic specific heat is

$$C_{en} = \gamma T, \quad \gamma \text{ is somerfeld constant}$$

Such an exponential dependence implies a minimum excitation per particle of $\sim 15 KT_c$.

2- The frequency threshold ω_0 for a sudden onset of absorption of infrared photons by thin superconducting films.

The above two experiments are consistent with a minimum energy Δ required to excite the superconducting specimen from the ground state. Completely similar effects, but with a vary different values of Δ are observed in insulators [8].

In insulators , Δ is of the order of an electron volt.

In superconductors, Δ is of the order of 10^{-3}ev , so that is of a few times $K_B T_c$.

In the BCS theory, it was shown that even a weak attractive interaction between electrons, such as that caused in second order by the electron - phonon interactions, causes

an instability of the ordinary Fermi-see ground state of the electron gas with respect to formation pound pairs of electrons occupying states with equal and opposite spin and momentum. These Cooper pairs have a spatial extension of the order of the coherence length (ξ_0), crudely speaking , comprise the superconductivity charge carriers anticipated in the theories (BCS theory).

One of the key predictions of the BCS theory was the minimum energy $E_g = 2\Delta(T)$ should be required to break a pair, creating two quasi particle excitation. This $\Delta(T)$ was predicted to increase from zero at T_c to limiting value such that [8]

$$E_g(0) = 2\Delta(0) = 3.528 KT_c \quad \text{for } T < T_c \quad (2.20)$$

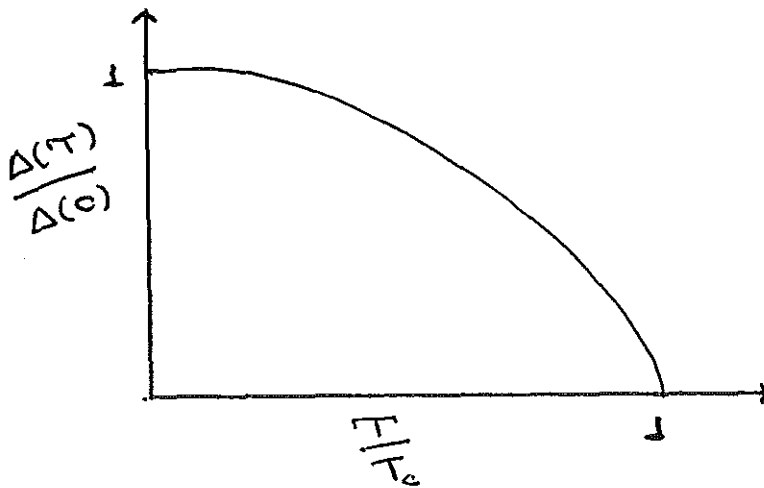


Fig 2.2 Temperature dependence of the energy gap in the BCS theory

$\Delta(T)$ can be computed numerically. For weak coupling superconductors, in which

$$\hbar\omega/KT_c \gg 1$$

$\Delta(T)/\Delta(0)$ is universal function of T/T_c which decreases monotonically from one at $T = 0$ to zero at T_c as in figure (2.2). Near $T = 0$, the temperature variation is exponentially slow. Physically speaking, $\Delta(T)$ is nearly constant until a significant of quasi - particle are thermally excited. On the otherhand, near T_c , $\Delta(T)$ drops to zero with a vertical tangent, approximately as

$$\Delta(T)/\Delta(0) \approx 1.74 (1 - T/T_c)^{1/2} \quad (T \approx T_c) \quad (2.21)$$

The temperature T_c at which the transition takes place is given from equation (2.11) as. [2]

$$KT_c = 1.13 \hbar\omega \exp\left(-\frac{1}{N(0)V}\right) \quad (2.22)$$

Since $\hbar\omega$ is proportional to $M^{\frac{1}{2}}$, from the dispersion relation equation (2.18), for a single element. This result gives immediately the isotope effect

$$T_c \sim M^{-1/2}$$

The gap parameter at the absolute zero is

$$\Delta(0) = 2\hbar\omega \exp\left(-\frac{1}{N(0)V}\right) \quad (2.23)$$

Hence, the ratio of energy gap at the absolute zero to $K T_c$ is a universal constant (BCS prediction)

$$2 \Delta(0)/KT_c = 3.53 \quad (2.24)$$

2.6 Josephson Effect

Josephson effect is the passage of paired electrons (Cooper pair) through a weak connection (Josephson junction) between superconductors, as in the tunnel passage of paired electrons through a thin dielectric layer separating two superconductors. [4]

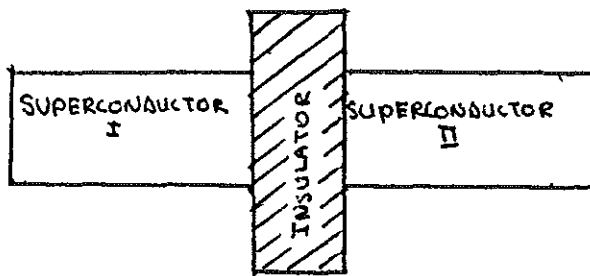


Fig 2.3 Josephson junction with two superconductors separated by an insulator

Josephson calculated the current that could be expected to flow during such superconductive tunneling and found that a current of paired electrons (super current) would flow in addition to the usual current that result, from the tunneling of a single electron.

In the absence of any electric field or magnetic field a dc current flows across the junction. This is known as Dc Josephson effect.

If a constant non - zero voltage V were maintained across the junction, an alternating super current would flow through the barrier - AC Josephson effect.

The frequency of the ac current is given by

$$\gamma = \frac{2ev}{h} \quad (2.25)$$

Where e is charge

h Planck's constant

In the quantum - mechanical description of a superconductor, all Cooper pairs in the superconductor have the same wave length and phase. It is this phase coherence that is responsible for the remarkable properties of the superconducting state. The common phase of the Cooper pairs in a superconductor is referred to as the phase of the superconductor.

The phase of two isolated superconductors are totally unrelated, while two superconductors in perfect contact have the same phase. If the superconductors are weakly connected (by a sufficient thin tunnel barrier), the phases can be different but not independent.

If ϕ is the difference in phase between superconductors on opposite sides of a tunnel barrier, the current through the junction is

$$I = I_0 \sin\phi \quad (2.26)$$

where, I_0 is critical current

The time dependence of the phase is given by

$$\frac{\partial\phi}{\partial t} = 2\pi \left(\frac{2eV}{h} \right) = 2\pi\gamma \quad (2.27)$$

For $V = 0$, ϕ is a constant

Integrating (2.27) shows the phase changes linearly in time for a constant voltage V , and the current will be

$$I = I_0 \sin [2\pi(2eV/h)t + \phi_0] \quad (2.28)$$

Some of the applications of the Josephson junction are redetermination of e/h , absolute temperature, voltage - frequency converter and based on this principle , superconducting quantum interference devices (SQUID) are constructed which consists of two Josephson contacts connected in parallel that can register changes of magnetic fields as small as 10^{-10} - 10^{-11} G.

Flux Quantization

Consider a superconducting ring, diameter and thickness much larger than the penetration depth. Experiments have shown that the flux ϕ , through the hole of the superconducting ring carrying a current appeared to be " quantized".

$$\phi = n\phi_0 \quad \text{where } n = 1, 2, 3, \dots$$

$$\phi_0 = ch/2e \approx 2 \times 10^{-7} \text{ G-cm}^2$$

The effective charge is $2e$, that is , the superconducting charge carriers are paired (Cooper pair) . This property, flux quantization , helps to construct computer memories.

CHAPTER IIIHIGH - Tc OXIDE SUPERCONDUCTORS3.1 The search for high - Tc superconductivity

Although the phenomenon of superconductivity was discovered more than 80 years ago, research on superconductivity has grown in importance for some decades. [12] The shortcoming of conventional superconductors is that they are characterized by low transition temperature. Hence, helium gas which is expensive and costly to liquify must be used to offer superconducting state. Since the discovery of superconductivity, materials have been searched which are characterized the highest possible transition temperature.

In 1986 Karl Alex Muller and Johannes Bednorz observe that an oxide of Barium, Lanthanum and Copper (La-Ba-Cu-O) might be superconductive at temperature up to 35°K. [13]

Since the initial discovery by Bednorz and Muller [12] of high temperature superconductivity, new breakthrough and advances in this field have continued at a furious pace. Within a span of a few months, the layered perovskite $\text{La}_{2-x}\text{Ba}_x\text{CuO}_{4-y}$ jumped to near 100°K in the distorted $\text{YBa}_2\text{Cu}_3\text{O}_{6+x}$ (1-2-3 compound) [14]

3.2 Structure of high - Tc oxides

In Y-Ba-Cu-O system, $\text{YBa}_2\text{Cu}_3\text{O}_{6+x}$ ($0 \leq x \leq 1$) the structure was proposed to be a distorted Oxygen deficient perovskite with ordering of Y and Ba ions in Ba - Y - Ba sequence along C - axis as in Fig 3.1

Perovskite is the mineral name of the oxide whose composition is CaTiO_3 , and whose structure consists of similar closest packed sheets of Calcium and Oxygen atoms containing

titanium at the center of the unit cubes. SrTiO_3 , BaZrO_3 , BaTiO_3 and others crystallize with this structure. [15]

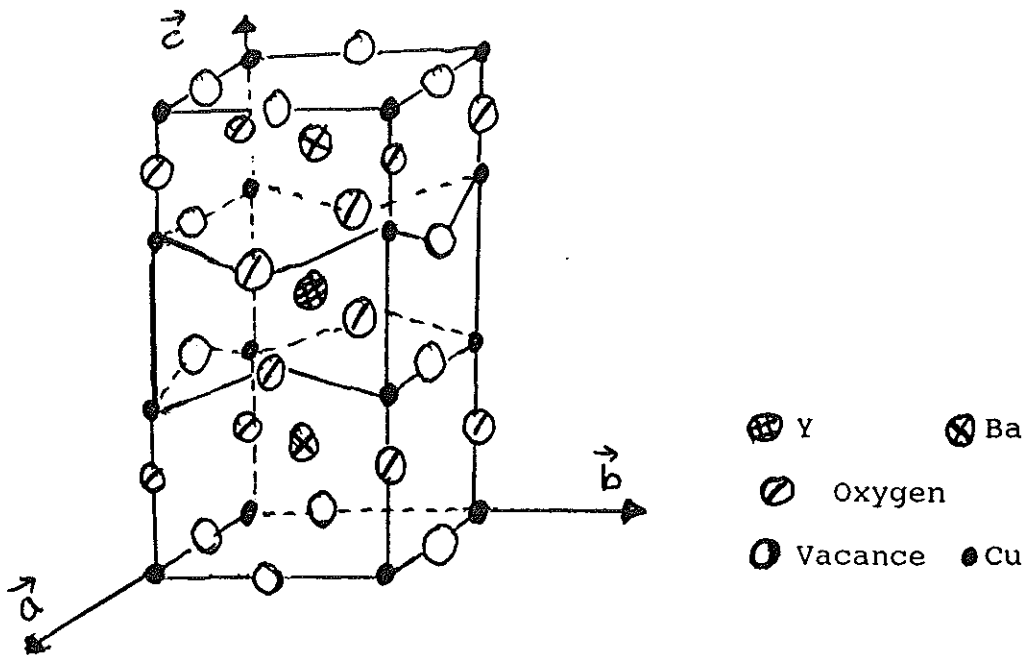


Fig 3.1 Model for $\text{Y}_1\text{Ba}_2\text{Cu}_3\text{O}_{6+x}$

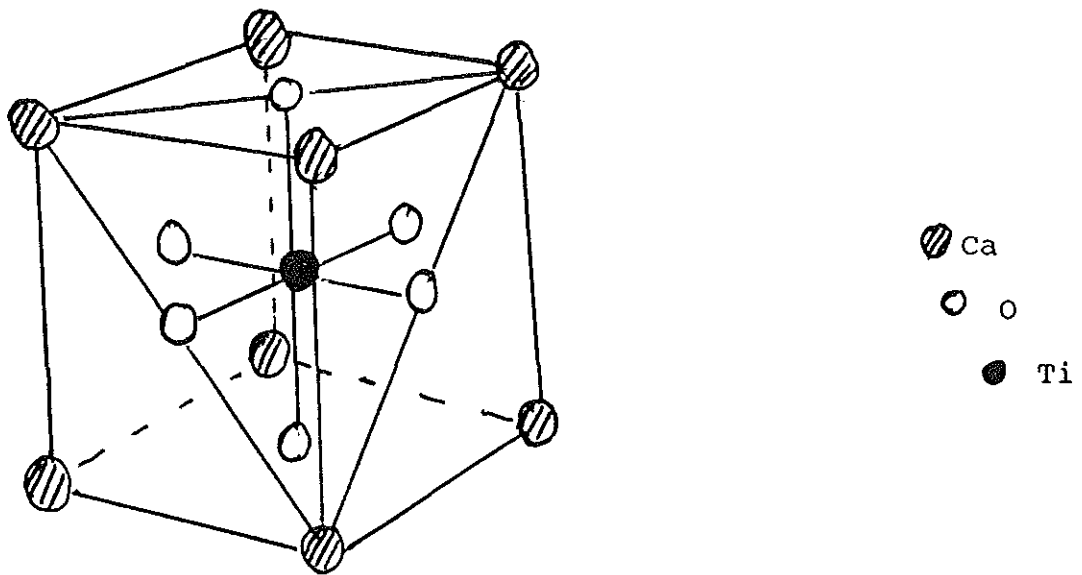


Fig 3.2 Perovskite (CaTiO_3) structure

The range of defect concentration in the compound is usually large, allowing the properties to be varied from insulating to superconducting [16].

For 1-2-3 compound ($\text{Y}_1\text{Ba}_2\text{Cu}_3\text{O}_{6+x}$)

Ortho - I phase with the 90 - K class T_c exists in the composition $X = 1 - 0.7$

Ortho - II phase with the 60 - K class T_c appears in the more oxygen deficient range $X = 0.7 - 0.5$

Below $X = 0.5$, the compound has a tetragonal structure and shows no superconductivity.

The superconductivity properties of $Y_1Ba_2Cu_3O_{6+x}$ depended generally on the conditions of preparation Sintering temperature, annealing temperature ... [17]

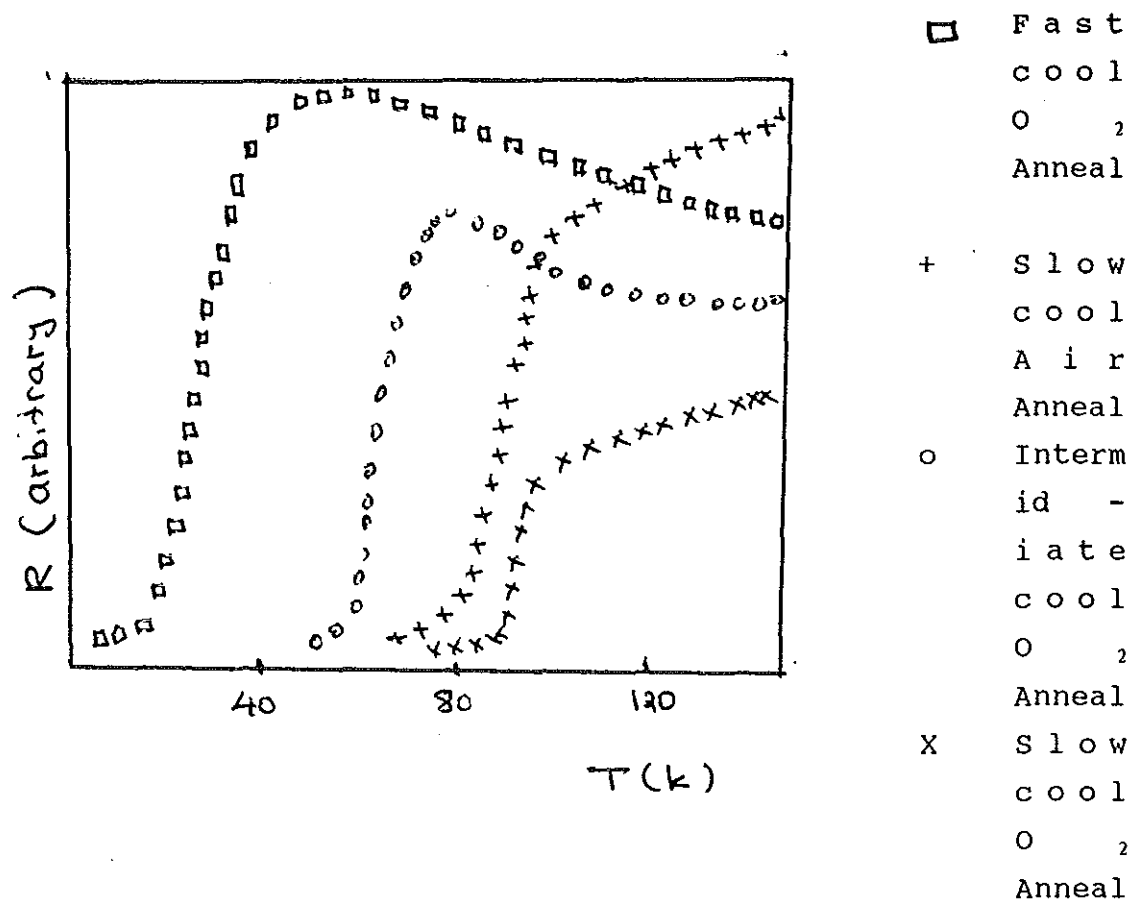


Fig 3.3 Resistance as a function of temperature for 1-2-3 compound at different conditions of preparations.

The highest and sharpest transition is obtained when the sample is heated in oxygen at 900° C and then allowed to cool slowing to room temperature over about 5 hours.

3.3 Charge - transfer model

The fact that T_c is unchanged by replacement of Y with the magnetic rare earth elements points to the Cu-O sublattice as the source of the superconducting properties of $Y_1Ba_2Cu_3O_{6+x}$ [16].

Mixtures of rare earths or alkaline earths also do not affect T_c , again emphasizing the key role of the Cu-O sublattice.

A natural model that arises from the common structural features of the copper oxides superconductors is that superconductivity occurs predominately in the CuO_2 planes, while the other (intercalated) layers provide, in some fashion, carriers or the coupling mechanism necessary for superconductivity. Such a model have come to be known charge - transfer model [19].

3.4 Physical Properties of Perovskite Oxides

The plasma reflectivity as well as the Hall and Seebeck effects have indicated that the carrier density is rather low in this family of oxides [19].

$Ln Ba_2 Cu_3 O_{6+x}$ with $Ln = Y$ and other rare earth elements, exhibit a sharp superconducting transition and an almost ideal Meissner effect measured by magnetic susceptibility. [as in Fig 3.4]

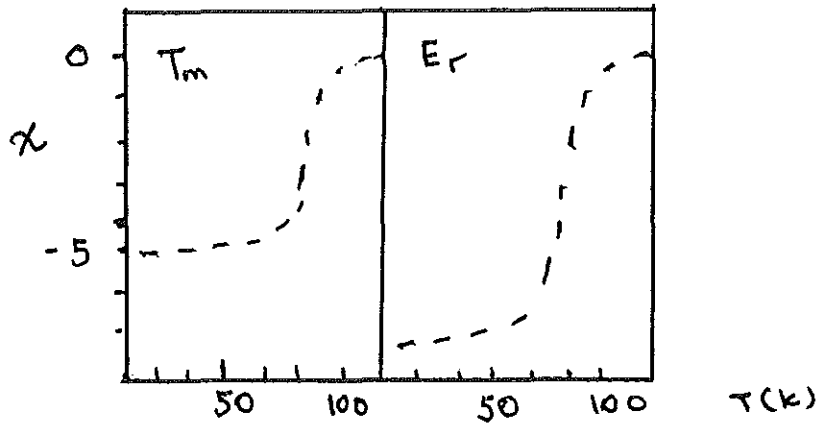


Fig 3.4 Flux - expulsion (Meissner) measurements in a field of 100 e for $TmBa_2Cu_3O_x$, and $ErBa_2Cu_3O_x$.

3.5 The Superconducting States in High - T_c Superconductors

From the experimental observation of the ac - Josephson effect, flux jump measurements , direct measurements the flux quantum ϕ_0 , it is found that Cuprate superconductivity involves the pairing of quasi particles (electrons), as expressed in an effective charge $e^* = 2e$

As in the conventional BCS theory the magnetic flux enclosed in a cavity of these materials is observed to be quantized in units of

$$\phi_0 = hc/2e \quad \text{where } h \text{ Plancks constant}$$

$$c \text{ speed of light}$$

$$e \text{ charge of electron}$$

This is a strong evidence that the charge are paired with charge $2e$. The pronounced layered structures of the cuprate influences electron properties, these compounds acts as

assembling of weakly coupled superconducting sheets. The values for the coherence length (ξ) and penetration depth (λ) parallel and perpendicular to the CuO_2 planes are deduced from measurements for 1-2-3 compounds in the low temperature limit are [19]

$$\xi_{ab} = 1.4 \pm 2 \text{ \AA}$$

$$\xi_c = 1.5 - 3 \text{ \AA}$$

$$\lambda_{ab} = 1400 \text{ \AA}$$

$$\lambda_c = 7000 \text{ \AA}$$

For comparison with conventional superconductors, (niobium), $\lambda = 350 \text{ \AA}$ and $\xi = 400 \text{ \AA}$

The length scales in the cuprates are rather extreme, thus they are extreme type II ($\lambda \gg \xi$) and are in the "clean" limit, i.e. $\xi(T=0)$ is much more less than the electronic mean-free path ($100 - 200 \text{ \AA}$) near T_c [20]

An external magnetic field can penetrate the cuprates to a relatively large (λ) depth because the few carrier density ($2.5 \times 10^{21} \text{ cm}^{-3}$) are not effective in shielding the field.

With the BCS pairing theory

$$\xi_0 = \hbar v_f / 2 \Delta(0)$$

v_f is Fermi velocity

$\Delta(0)$ is the superconducting gap

ξ_0 of 15 \AA is indeed consistent with $v_f = 1.1 \times 10^7 \text{ cm/sec}$ and $2\Delta(0) = 6k_B T_c$, which are typical parameters for 1-2-3 compounds.

Since the coherence length ξ_c perpendicular to the CuO_2 is only few angstrom, the superconducting layers are weakly coupled.

3.6 Superconducting Gap

In the superconducting state a minimum energy 2Δ , the gap energy, is required to break up a superconducting (cooper) pair. No electronic excitations are possible below the gap.

In conventional superconductors, Δ is isotropic, in cuprates, variety of measurements indicates that the true gap exists every where on the Fermi surface i.e $\Delta(K) \neq 0$ for all K.

[19]

Electron tunneling, high - resolution photoemission spectroscopy, optical spectroscopy and Raman scattering are some of the techniques which can be employed to measure the magnitude and temperature dependance of the superconducting gap $\Delta(T)$

The results common to these studies is of a $2\Delta/K_B T_c$ ratio that tends to be in the range 5 to 8, and hence larger than the weak coupling BCS value 3.5.

3.7 High - Tc Oxide Superconductor without a Rare - Earth Element

After the discovery of high - Tc superconductors with Tc around 90 K in 1-2-3 compounds. No new stable superconductors with Tc higher than that of $Y_1Ba_2Cu_3O_7$, have been reported in Y-Ba-Cu-O system. The values have not improved by the substitution of other rare earth elements for yttrium.

In order to find high Tc superconductors, it was important to investigate other classes of oxide systems including the V_b - element group such as Bi and Sb of trivalent elements, namely $BiSrCaCu_2O_y$, with Tc of about 100 K by Maeda et al [20]

The value of Tc in the Bi - Sr - Cu - O oxide system which

does not include Ca is very low about 8K [22] In order to obtain high T_c , the coexistence of Sr and Ca in the Bi oxide system is found to be absolutely necessary.

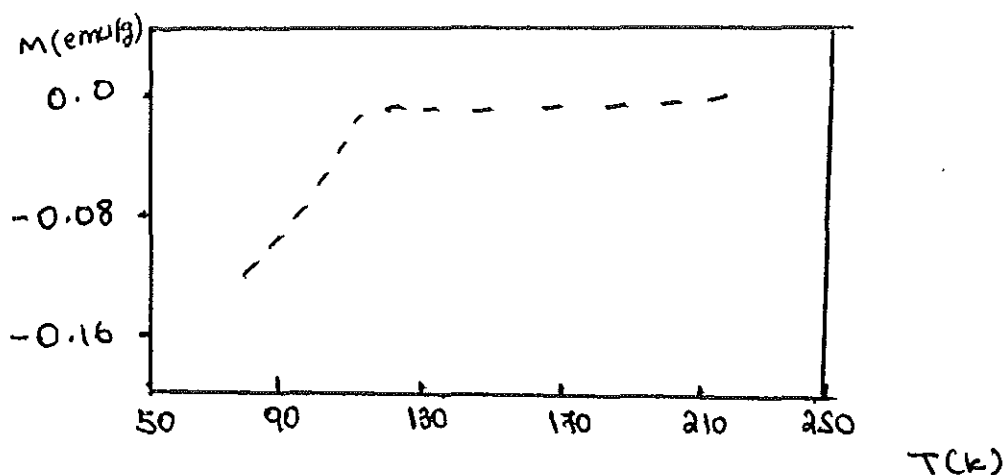


Fig 3.5 (Meissner effect) Magnetization as function of temps. [21]

After the discovery of high - T_c superconductors in the Bi - Sr - Ca - Cu - O system, intensive studies of phase identification , physical and chemical properties have been carried out for the compounds of $\text{Bi}_2\text{Sr}_2\text{Ca}_1\text{Cu}_2\text{O}_x$ with $T_c = 80$ K 2212 phase and $\text{Bi}_2\text{Sr}_2\text{Ca}_1\text{Cu}_2\text{O}_x$ with $T_c = 100$ °K (2223 phase) [22]

2223 phase is a member of the group which has the highest T_c [20] , and contains triple CuO_2 layers in the unit cell.

The Bi composition included many phases with various composition and it was very difficult to obtain a high - T_c single phase. The introduction of Pb , i.e $(\text{Bi,Pb})_2\text{Sr}_2\text{Ca}_2\text{Cu}_3\text{O}_x$, is a good single - phase in an easily reproducible way.

3.8 Isotope Effect in the high - T_c Superconductors

It is well known that the effect of isotope substitution on the superconducting transition , T_c , provides the strongest

support for the mechanism that phonons are involved in the formation of the superconducting state, in the framework of the BCS theory.

For the case of the high - T_c oxide superconductors, central to the conventional model are the high frequencies of the Cu-O bond - stretching vibrational modes and their strong coupling to the electronic state of the Fermi level, presumed to be the result of strong mixture of oxygen p state with the Cooper states at the Fermi level. The high - frequency modes involve the motion of oxygen atoms and thus replacement of ^{16}O by ^{18}O may be expected to modify significantly the vibrational mode frequencies, which in turn should affect the superconducting T_c .

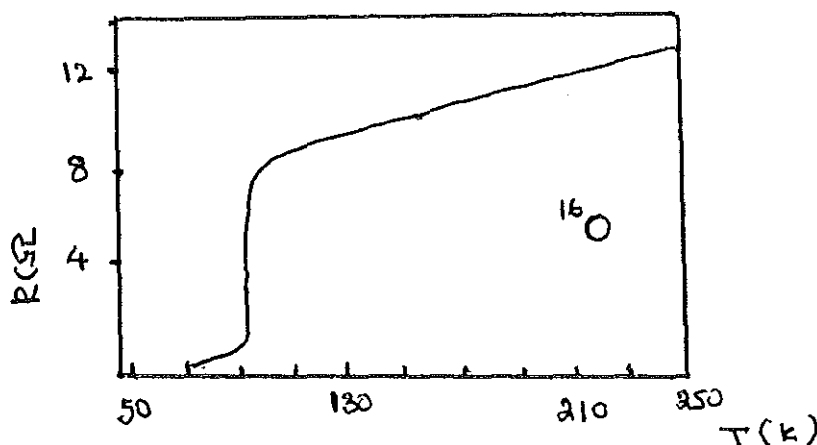
The high frequency vibrational modes were characterized by Raman spectroscopy, clearly showing the expected mass dependent shift. There is, however, no significant variation in the superconducting T_c as in Fig 3.6 [23].

The mass dependent of T_c is generally expressed as

$$T_c \sim M^\alpha$$

Where M is isotopic mass

α is constant usually close to 0.5 for the full isotope effect.



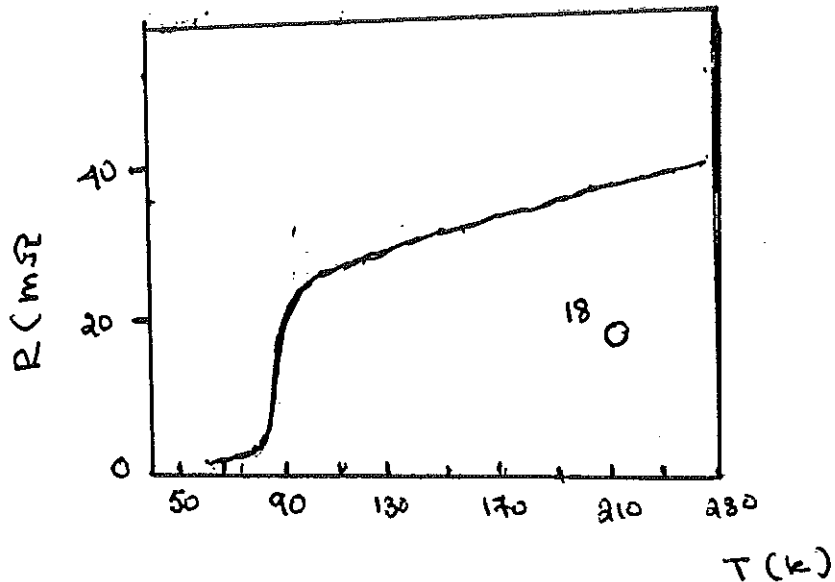


Fig 3.6 R Vs T for 1-2-3 compound with ^{16}O and ^{18}O . No isotope effect is observed [23]

It has been searched for an isotope effects in $\text{YBa}_2\text{Cu}_3\text{O}_{6+x}$, by substituting the isotope ^{18}O for ^{16}O , no shift in T_c is observed in either dc electrical resistivity measured or dc magnetic susceptibility measurements. This result shows that [23,24]

$$\alpha = 0.0 \pm 0.0027$$

The oxygen isotope effect is absent in superconducting Y-Ba-Cu-O. This suggests that although the BCS phonon mechanism may still be appropriate for explaining the high - T_c superconducting behavior. The absence of an oxygen isotope shift suggests that a non - phonon mechanism may be important in these materials.

3.9 Exciton Mechanism of superconductivity [24,27]

The Exciton mechanism of superconductors is a mechanism, in which the effective attraction interaction between electrons comes from virtual excitations of excitons (electron hole pairs) rather than phonons. The importance of this mechanism is emphasized because of the possibility of obtaining higher transition temperatures than can be realized through the phonon mechanism.

An electron from the fermilevel of the metal may tunnel to the semiconductor layer and exciting an electron from the valence band of the semiconductor creating an electron hole pair (exciton) which are bound by their attractive electrostatic interaction.

Exciton can be discussed in two different limiting approximations, one by Frenkel in which the exciton is small and tightly bound, and the other by Mott and Wannier in which the exciton is weakly bound, with an electron - hole separation large in comparison with a lattice constant [4]. For the case of high T_c oxide superconductors the excitons, out of theoretical reasoning, are Mott excitons.

The exciton mechanism of superconductors is discussed with respect to a particular model [24], ABB (David Allender, James Bray and John Bardeen). - a thin metal layer on a semiconductor surface, the metal electrons at the Fermi - surface tunnel in to the semiconductor gap where they interact with virtual excitons, producing a net attractive interaction among the electrodes in direct analog with the phonon mechanism of superconductivity [25]

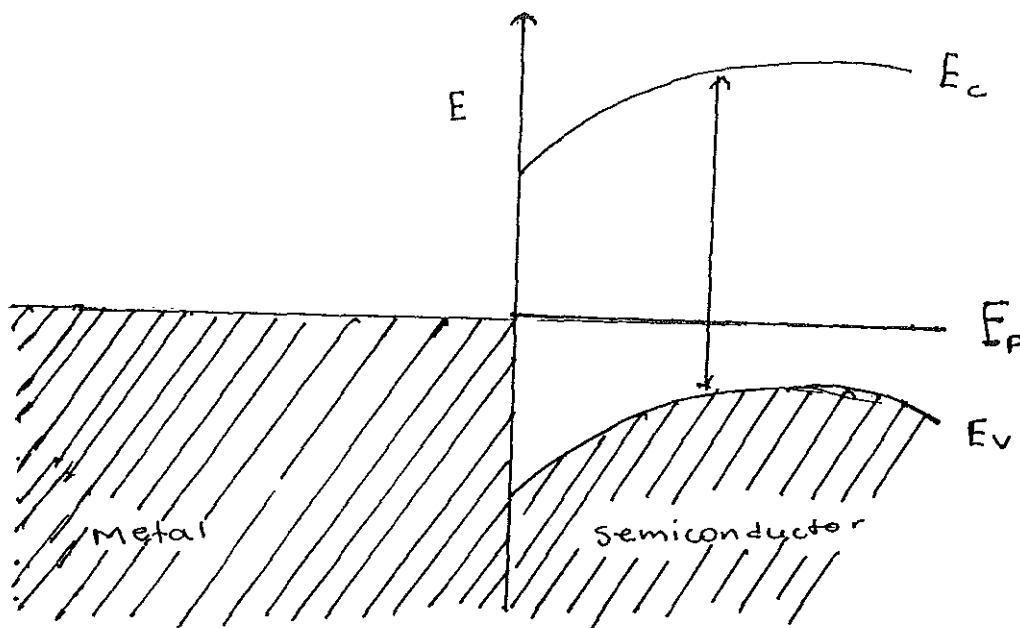


Fig. 3.7 Energy band diagram for Metal - Semiconductor interface (ABB model)

As is well known from BCS theory of superconductivity, an attractive interaction between electrons near the Fermi surface in a material is necessary for a superconducting state to exist. For a metal - semiconductor system, the interaction is the combination of three contributions,

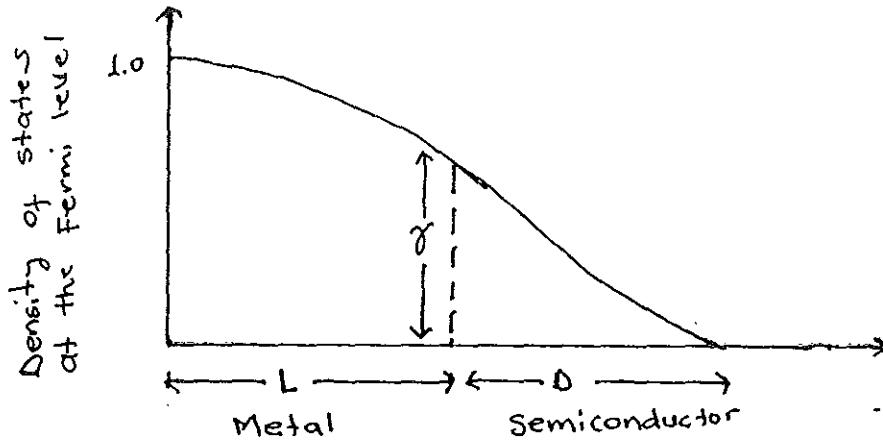
$$V(W) = V_{ph} + V_c + V_{ex}$$

Where V_{ph} is the phonon part

V_c is the coulomb interact

V_{ex} is the exction part.

$\hbar\omega$ - variables is an energy variable representing the energy difference between the initial and final states which occurs in the matrix elements for the scattering process.



the density at the interface is given by $\gamma N(0)$, $\gamma \sim \frac{1}{2}$
 L , D , thickness of the metal and semiconductor respectively
 The coulomb interaction is

$$V_c(q, w) = 4\pi e^2 / (q^2 \epsilon(q, w))$$

$$\cong 4\pi e^2 / (q^2 + q_s^2) \quad \text{for } w \ll w_F \quad (3.1)$$

Where $q, \hbar w$ are the momentum and energy transfers in the electron scattering, $\epsilon(q, w)$ is the electronic dielectric function for a metal of equivalent electron and q_s is an appropriate screening wave vector density. we may then define μ to be the average of $V_c(q, w)$ over the Fermi surface times the density of states at the Fermi surface $N(0)$:

$$\mu = N(0) \langle V_c \rangle \quad (3.2)$$

The average over the fermi surface $\langle V_c \rangle$, may be expressed as an integral over q , leaving in as a function of w only, we then choose the square - well model, in which μ is taken to be constant out to be

$$w = w_F: \quad \mu(w) = \mu \quad \text{for } 0 \leq |w| \leq w_F$$

$$= 0 \quad \text{otherwise}$$

Typical values for μ is of the order 0.2 - 0.5. The phonon interaction may be described by λ_{ph} , and we shall adopt the definition of λ_{ph} from McMillan [25]

$$\lambda_{ph} = 2 \int_0^{w_{pm}} \alpha^2(w) \frac{F(w)}{w} dw \quad (3.3)$$

Where $\alpha^2(w)$ is an average matrix element of the phonon interaction,

$F(w)$ is the phonon density of states

w_{pm} is the maximum phonon energy.

Next we derive an estimate of the exciton - electron coupling constant λ_{ex} .

The interaction term in the Hamiltonian for a metal electron arising from the semiconductor electrons consists of a screened coulomb - like potential, summed over all of the semiconductor valence electrons; where

$$H_{int} = \sum_i \frac{e^2}{|r_i - r|}, \quad (3.4)$$

Where r is the coordinate of the metal electron and r_i is the position of the i^{th} semiconductor - valence electron. The superscript implies that the interaction is screened as in a metallic Jellium model of equivalent electron density.

We Fourier transform to obtain , for $w \ll w_F$

$$H_{int}(r) = \sum_i \sum_q \frac{4\pi e^2}{(q^2 \epsilon(\vec{q}, w=0))} e^{i\vec{q} \cdot \vec{r}_i - i\vec{q} \cdot \vec{r}} \quad (3.5)$$

$4\pi e^2/q^2 \epsilon$ is the fourier coefficient of the screened interact.

equation (3.5) can be written as

$$H_{int} = \sum_q S (4\pi e^2/q^2) p_q \cdot e^{-iqr} \quad (3.6)$$

Where $P_q \equiv \sum_i e^{iqr_i}$

S is the screening factor of order $\frac{1}{2}$ and approximates the

effects of the dielectric tensor $1/\epsilon$. $S = \langle 1/\epsilon \rangle$

we form the matrix element

$$M = \langle N, \vec{K}_2 | H_{int} | 0, \vec{K}_1 \rangle \quad (3.7)$$

Where $|0, K\rangle$ is the initial state with no excitation and a metal electron of momentum \vec{K}_1 and $|N, \vec{K}_2\rangle$ is the final state with an exciton $|N\rangle$ of definite momentum $-q$ and the metal electron scattered to $\vec{K}_2 = \vec{K}_1 + \vec{q}$

If we assume plane - wave states for the metal electrons, the matrix element becomes

$$M = \sum_q S (4\pi e^2/q'^2) (p_q)_{N0} \delta_{qq'} \quad (3.8)$$

Where $(p_q)_{N0} \equiv \langle N | p_q | 0 \rangle$

Since either pair of electron may emit or absorb the exciton we will introduce additional factor 2. Thus for $w \ll w_{N0}$

$$V_{ex} = 2 \sum_N |M|^2 / w_{N0} \quad (3.9)$$

or in terms of the fraction of time the metal electrons are in semiconductor (b) and the decreased amplitude in the penetration depth

$$V_{ex} = 2S^2 4\pi e^2/q^2 \sum_N \gamma b 4\pi e^2/q^2 (p_q)_{N0}^2 / w_{N0} \quad (3.10)$$

approximating w_{N0} by $\langle w_{N0} \rangle = w_q$ - the average gap width.

$$V_{ex} = 2S^2 \gamma b (4\pi e^2/q^2 w_q) \sum_N 4\pi e^2/q^2 (p_q)_{N0}^2 / w_{N0} \quad (3.11)$$

using the following two sum rules [27]

$$\begin{aligned} \int_0^\infty \omega \epsilon_2(\omega) d\omega &= \frac{1}{2} \pi \omega_p^2 = \frac{1}{2} \pi \left(\frac{4\pi N_e e^2}{m} \right) \\ \int_0^\infty \epsilon_2(\omega) d\omega &= \sum \left(\frac{4\pi^2 e^2}{q^2} \right) (P_q)_{N0}^2 \end{aligned} \quad (3.12)$$

where w_p is the electronic plasma frequency

ϵ_2 is the imaginary part of the dielectric function,

n_c is the density of semiconductor valence electrons.

The first sum rule can be approximate assuming that ϵ_2 is sharply peaked at $w = w_g$, and integrating just over this

exction peak $\int_0^{\infty} \omega \epsilon_2(\omega) d\omega \rightarrow \omega_g \int_{peak} \epsilon_2(\omega) d\omega$

we may reduce n_c to some value n_{eff} to account over the exciton peak, then

$$\begin{aligned} \int_{peak} 1/\omega_g \epsilon^2(\omega) d\omega &= (1/2\pi) \omega_p^2/\omega_g^2 \\ &= 1/\omega_g \sum 4\pi^2 e^2/q^2 (p_q)_{N_0}^2 \end{aligned}$$

giving

$$V_{ex} = S^2 \gamma b \mu \frac{\omega_p^2}{\omega_g^2} \quad (3.13)$$

The value of λ_{cx} is $N(0)$ times the average of V_{cx} over the Fermi surface [25].

$$\begin{aligned} \lambda_{cx} &= N(0) \langle V_{cx} \rangle \\ &\approx [N(0) \langle S(4\pi e^2/q^2) \rangle \langle S \rangle \gamma b (w_p^2/w_q^2)] \\ \lambda_{cx} &= S \gamma b \mu (w_p^2/w_q^2) \quad \text{since } \mu = N(0) \langle S(4\pi e^2/q^2) \rangle \end{aligned}$$

Or

$$\lambda_{cx} = a b \mu (w_p^2/w_q^2) \quad (3.14)$$

Where $a = S \gamma$

ABB treat superconductivity at a metal semiconductor interface where the " electron - electron cooper pair" can be bound through a phonon and/or an exciton. We know that the

latest high T_c oxide superconductors, are sandwich structures with alternating layers of metal-semiconductors -metal-semiconductors, etc . Which can be described by the theory of ABB.

From ABB we have

$$T_c = (0.7) \theta_0 \exp [-1/g_{eff}] \quad (3.15)$$

where θ_0 is related to the Debye temperature and is given by

$$\theta_0 = \hbar w_{po}/K_B$$

K_B is the Boltzmann constant

w_{po} is the maximum phonon frequency

\hbar is planck's constant by 2π

Here

$$g_{eff} = \lambda_{ph}^* + (\lambda_{ex}^* - \mu') / \{ 1 - (\lambda_{ex}^* - \mu') \ln(w_g/w_{po}) \}$$

Where

$$\lambda_{ph}^* = \lambda_{ph} / (1 + \lambda_{ph})$$

λ_{ph} is the electron - phonon coupling constant , and

$$\lambda_{ex}^* = \lambda_{ex} / (1 + \lambda_{ex})$$

λ_{ex} is the electron - exciton coupling constant

Where μ is the average of states times an average of the screened coulomb interaction, w_g is the average semiconductor energy gap, and w_F is the fermi energy given by

$$w_F = (\hbar^2/2m^*) (3\pi^2 N)^{2/3} \quad , \text{ For a simple parabolic band}$$

N - is the carrier density

m^* - is the effective mass

In order to make these equations more transparent to analyze the isotope experiments with ABB's " phonon + exciton " theory

, we introduce the approximation [28]

$$\lambda_{ph}^* \ln(w_g/w_{p0}) \ll 1 \quad (3.16)$$

Thus,

$$T_c \cong 0.7\theta_0(\theta_{ex}/\theta_0)^{(\lambda_{ex}^* - \mu')/(\lambda_{ph}^* + \lambda_{ex}^* - \mu')^2} \exp(-1/\lambda_{ph}^* + \lambda_{ex}^* - \mu') \quad (3.17)$$

Where $\theta_{ex} = w_g/K_B$ is the "excitonic temperature" which is a more accurate description of the excition formation energy than the band gap (w_g)

To examine isotope effect

$$\theta_0 \propto M^{-1/2}$$

In equation (3.17) all other terms are independent of isotopic mass

Thus

$$T_c \propto M^{-1/2 [1 - ((\lambda_{ex}^* - \mu')/(\lambda_{ph}^* + \lambda_{ex}^* - \mu'))^2]} \quad (3.18)$$

It is clear that minimal isotopic effect can be obtained when the exciton mechanism is dominant

$$\lambda_{ex}^* \gg \lambda_{ph}^*$$

$$T_c \propto M^{-1/2 [1 - ((\lambda_{ex}^* - \mu')/(\lambda_{ex}^* - \mu'))^2]}$$

$$T_c \propto M^0$$

The transition temperature is independent of isotopic mass. We can say that , an excitonic mediated mechanism may be primarily responsible for the high transition temperature superconductivity is Y - Ba - Cu - O rather than a phonon mechanism.

Proceeding with the excitonic mechanism, the expression for λ_{ex}

$$\lambda_{ex} = b\mu w_p^2 / w_g^2$$

Taking favorable estimate

$$w_p \approx 10 \text{ ev}$$

$$w_g \approx 12 \text{ eV}$$

$$a \approx 1/3 - 1/5$$

$$\mu \approx 1/3 - 1/2$$

$$b \approx 0.2$$

give values for $\lambda_{ex} \approx 0.2$ to 0.5 (3.19)

Considering the value of λ_{ex} in equation (3.19), superconductors with transition temperature around 40 K are explainable. The results are shown in Fig 3.8.

Estimate for $Y_1Ba_2Cu_3O_7$ indicates that higher values are reasonable

$$\lambda_{ex} \approx 1.0 - 1.5 \quad (3.20)$$

Here, the dependence of λ_{ex} on free carrier density N can be considered as

$$b \propto N^{1/3}$$

$$\lambda \propto N^{-1/4}$$

Which finally yields

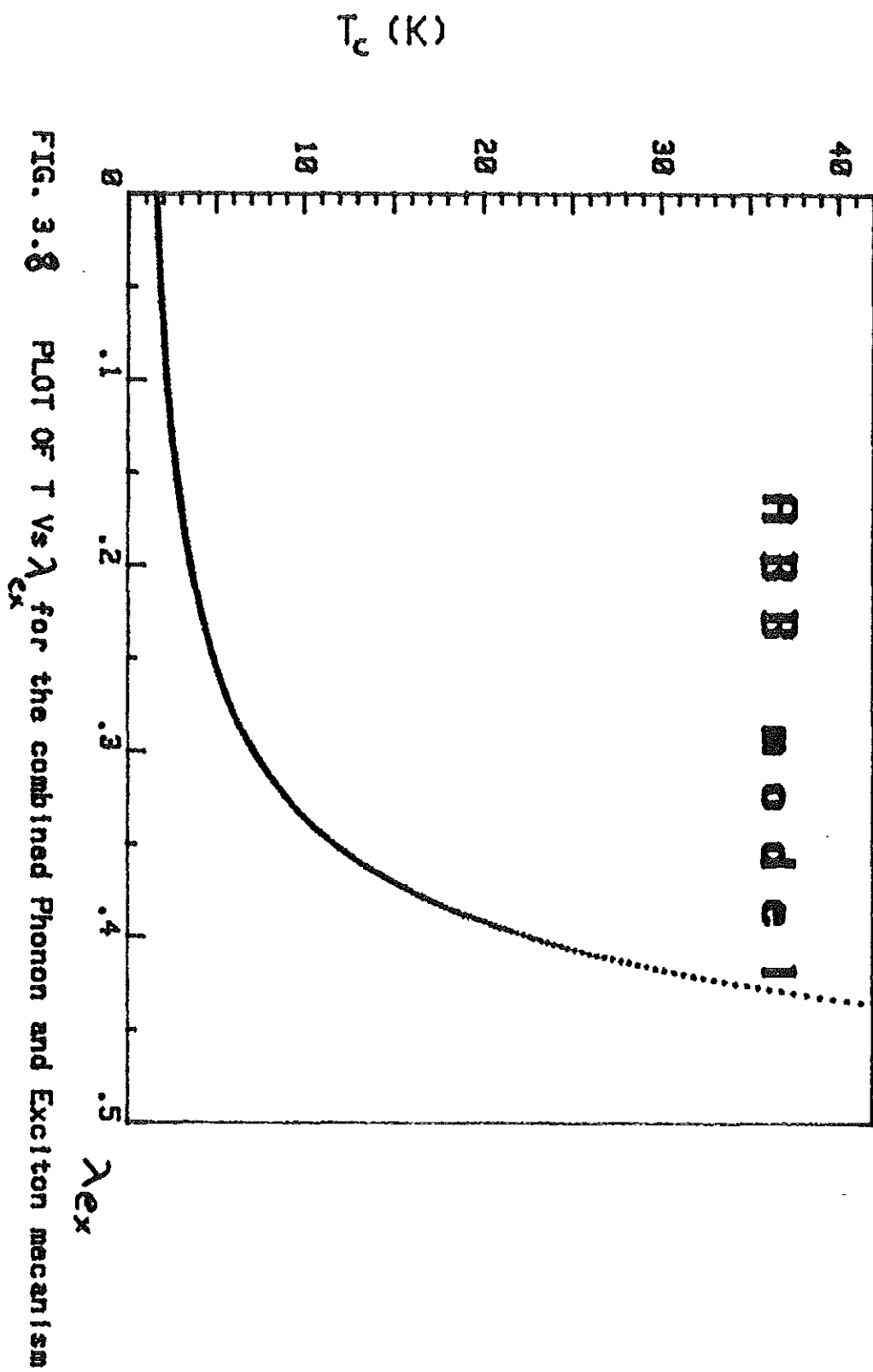
$$\lambda_{ex} = [(0.85) \times 10^{-21} \text{ cm}^3 \text{ N}]^{0.22} \quad (3.21)$$

The Debaye temperature was taken approximately 600 K. Other parameters were estimated from ABB

$$w_g = 0.16 \text{ eV} \quad , \quad \mu = 1/3$$

$$m^* = 3 \quad , \quad \lambda_{ph} = 0.015$$

For these parameters, it was found that λ_{ex} varies up to 1.7 as in fig. (3.9) and the theoretical curve for T_c as function of log carrier concentration is given in Fig. (3.10).



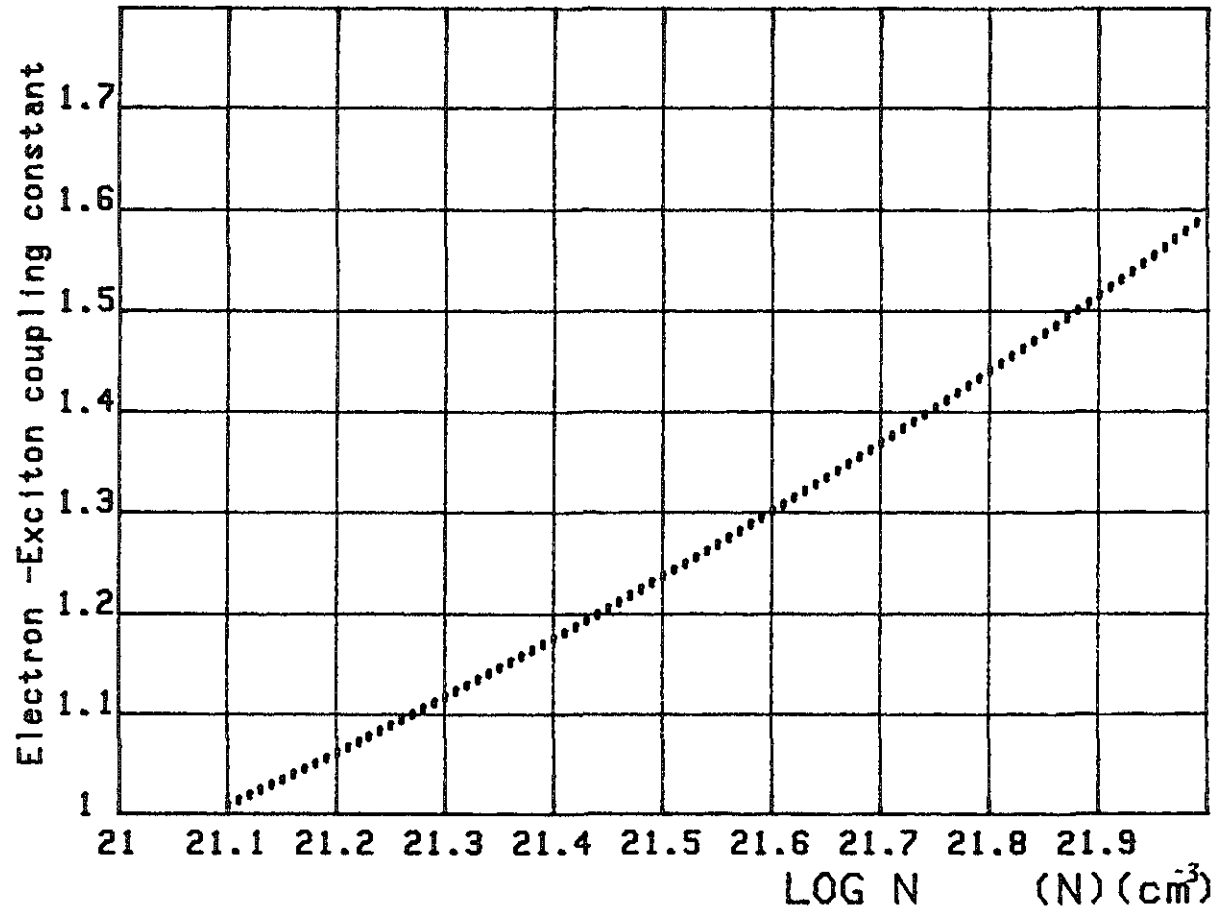


Fig. 3.9 Theoretical values of Electron - Exciton coupling parameter Vs carrier concentration

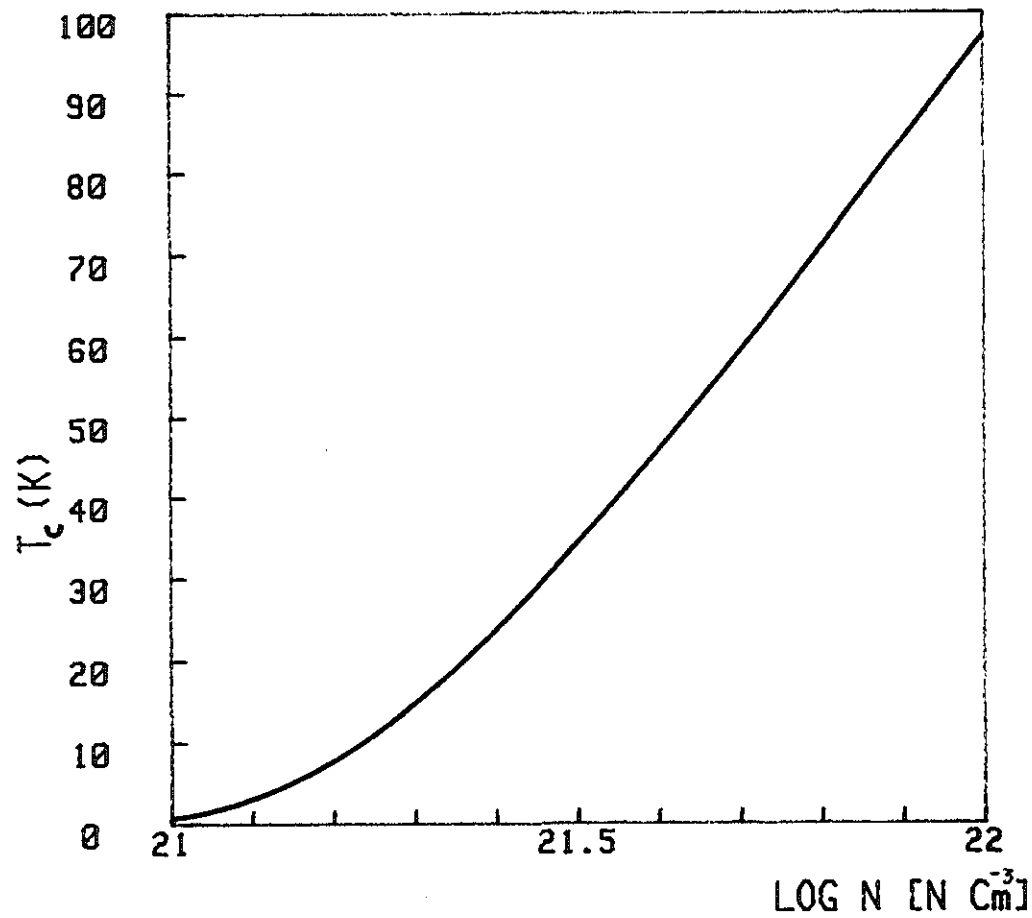


Fig. 3.10 T_c as function of log carrier concentration for oxide superconductors

CHAPTER IV

EXPERIMENTAL STUDY ON 123, 2212 AND 2223 PHASES OF OXIDE
SUPERCONDUCTORS.4.1 Sample Preparation4.1.1 1-2-3 Compound ($Y_1Ba_2Cu_3O_7$)

The raw materials of $BaCO_3$, Y_2O_3 , CuO are mixed in their appropriate ratios by ball-milling for 24 hours. The solid state reaction of the mixture are performed by heating at $900^\circ C$ for 6 hours. After the ball-milling for 48 hours again, the products are pressed into pellets. The pellets are sintered directly at varied tempratures ($1024-1140^\circ$) for different duration of time (4-9 hours) in air or Oxygen [28].

4.1.2 2-2-1-2 Phase ($Bi_2Sr_2CaCu_2O_{11}$)

The specimen was synthesized by a solid state reaction from Bi_2O_3 , $SrCO_3$, $CaCO_3$ and CuO . The stoichiometric mixtures was ground and pelletized. The pellet was heated in air at $800^\circ C$ for 20 hours then cooled at a rate of $8^\circ C$ per hour, followed by cooling to room temprature in the furnace [29].

4.1.3 2-2-2-3 phase [$(Bi,Pb)_2Sr_2Ca_2Cu_3O_{11}$]

The sample could be prepared by an ordinary solid-state reaction method. Powders of Bi_2O_3 , Pb_3O_4 , $SrCO_3$, CuO were mixed with typical ratio, calcinated at $830^\circ C$ for 20 hours, and pressed in to pellets. The pellets were sintered at $860 - 870^\circ C$ for 50 - 100 hours in air [30].

4.2 Structure Investigation

The structure of high - T_c superconductors can be studied

at room temperature by X-ray diffraction technique. The X-ray diffraction intensity data of samples were collected on x-ray diffractometer. Operating conditions are : Cu - K_{α} at 40 Kv and 50 mA, and the source wave length is 1.57\AA .

So far, the crystal structure were studied. We tried only to compare our data with other's results. They are similar to that of published ones [32].

Comparing our pattern, in Fig 4.1, Fig 4.2 and Fig 4.3, with published results, the lattice parametres are [32]

	a(\AA)	b(\AA)	c(\AA)
For 123 phase	3.877	3.824	11.69

The lattice of this phase (123 phase) is closely related to the orthorhombic perovskite structure. 123 phase exists in orthorhombic and tetragonal form, tetragonal structure shows no superconductivity [31]

	a(\AA)	c(\AA)
For 2223 phase	5.43	37.1

This phase is tetragonal perovskite structure.

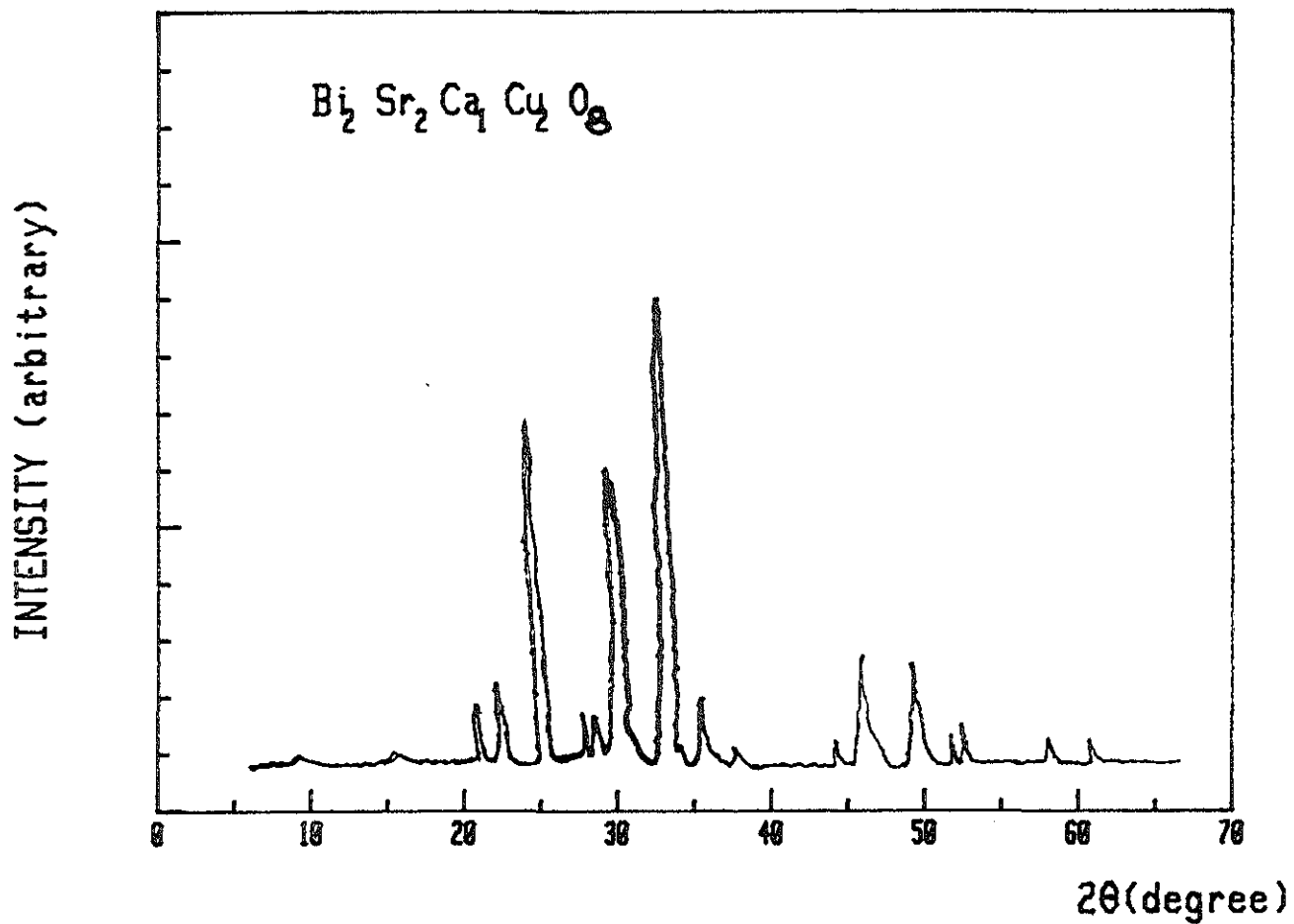


Fig. 4.1 X-ray diffraction pattern of 2212 phase with Cu-K_α radiation

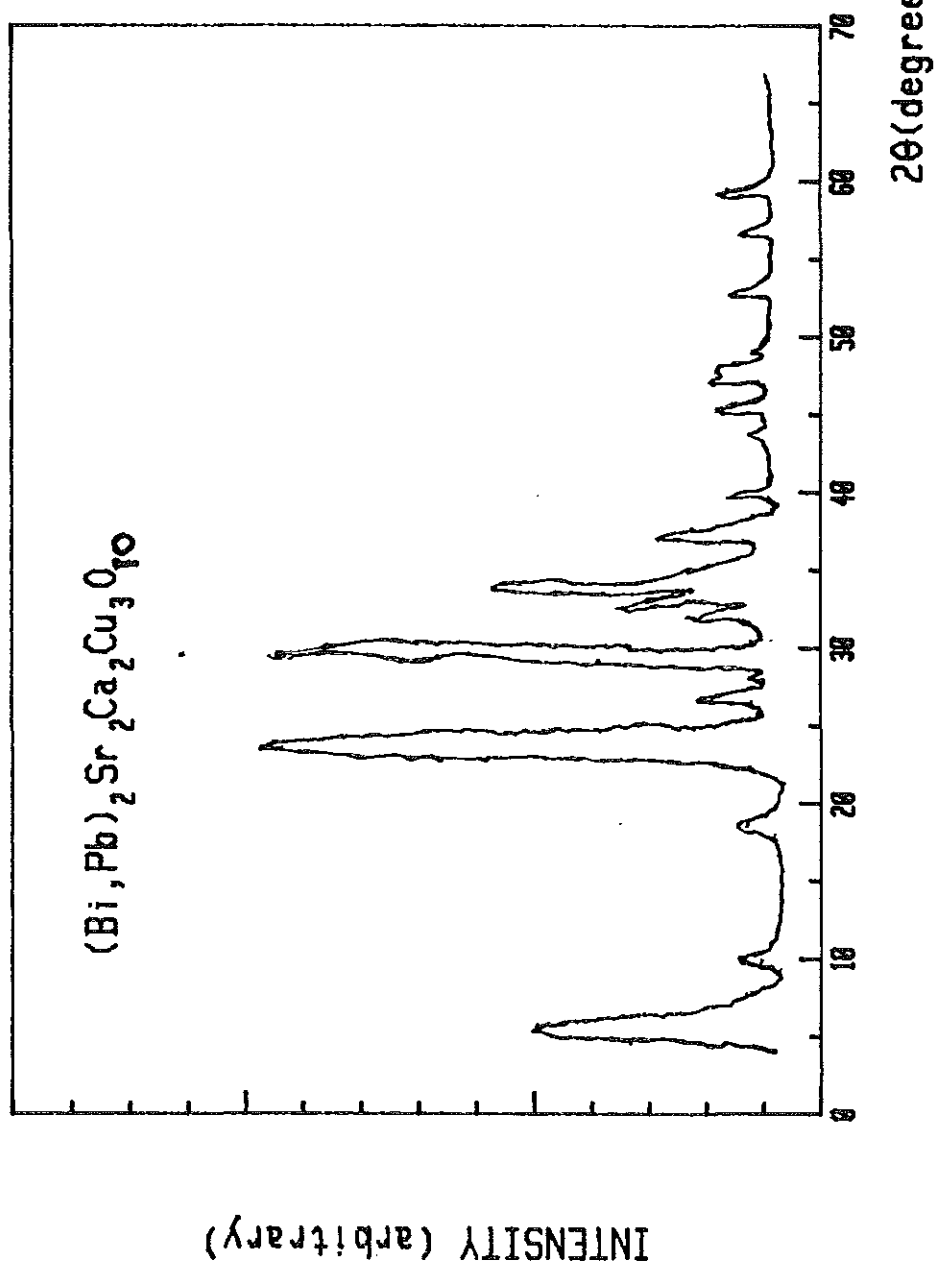


Fig. 4.2. X-ray diffraction pattern of 2223 phase with $\text{Cu-K}\alpha$ radiation

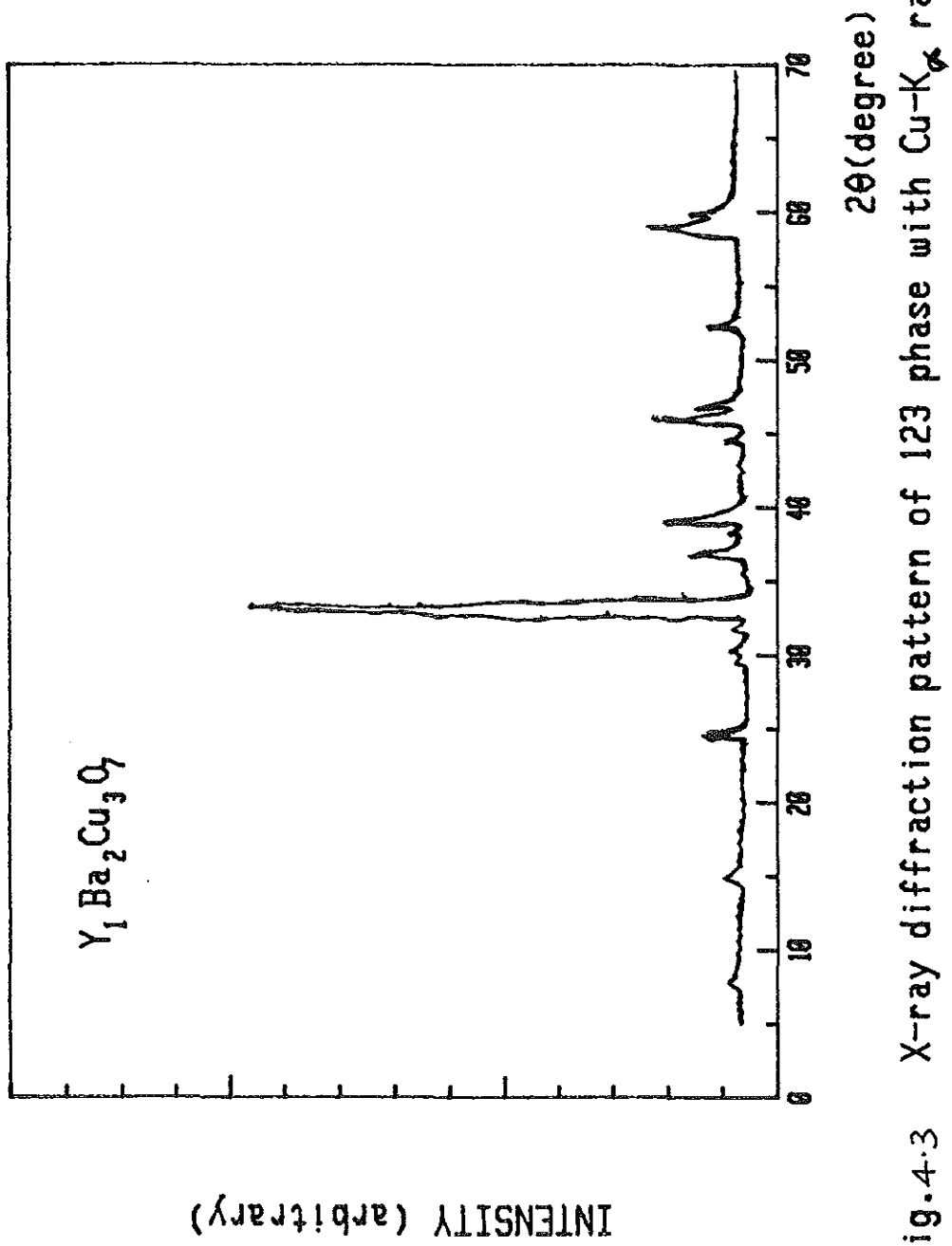
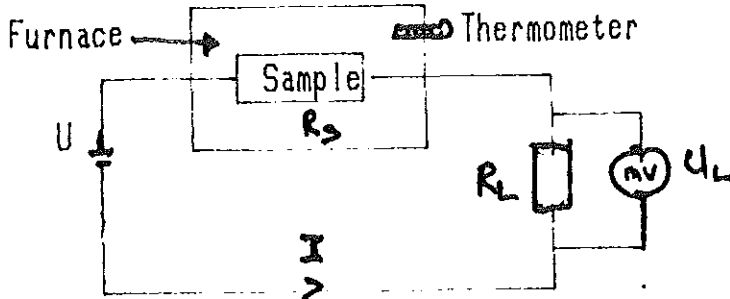


Fig.4.3 X-ray diffraction pattern of 123 phase with Cu-K α radiation

4.3 Investigation of Resistance Dependence on Temperature

4.3.1 Two - Probe Method



where R_s is sample resistor

R_L is load resistor

U_0 is applied voltage

U_L is load voltage

Fig. 4.4 Experimental set up for two - probe

In investigating the resistance dependence on temperature, the sample was placed inside a furnace and the temperature reading were measured by thermometer and the resistance was measured by measuring the potential drop across the sample by passing a constant current, hence the resistance. Since voltage is directly related to resistance for a constant current.

4.3.2 Four - Probe Method

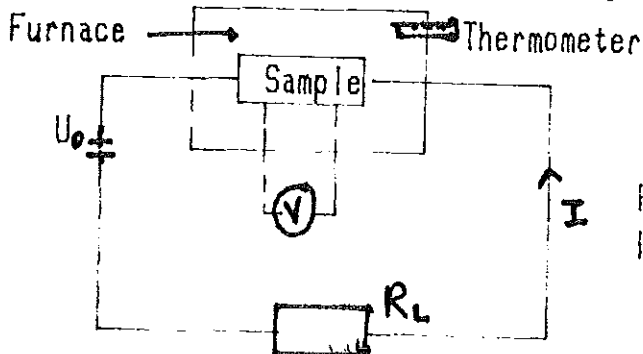


Fig 4.5 Experimental set up for Four - probe

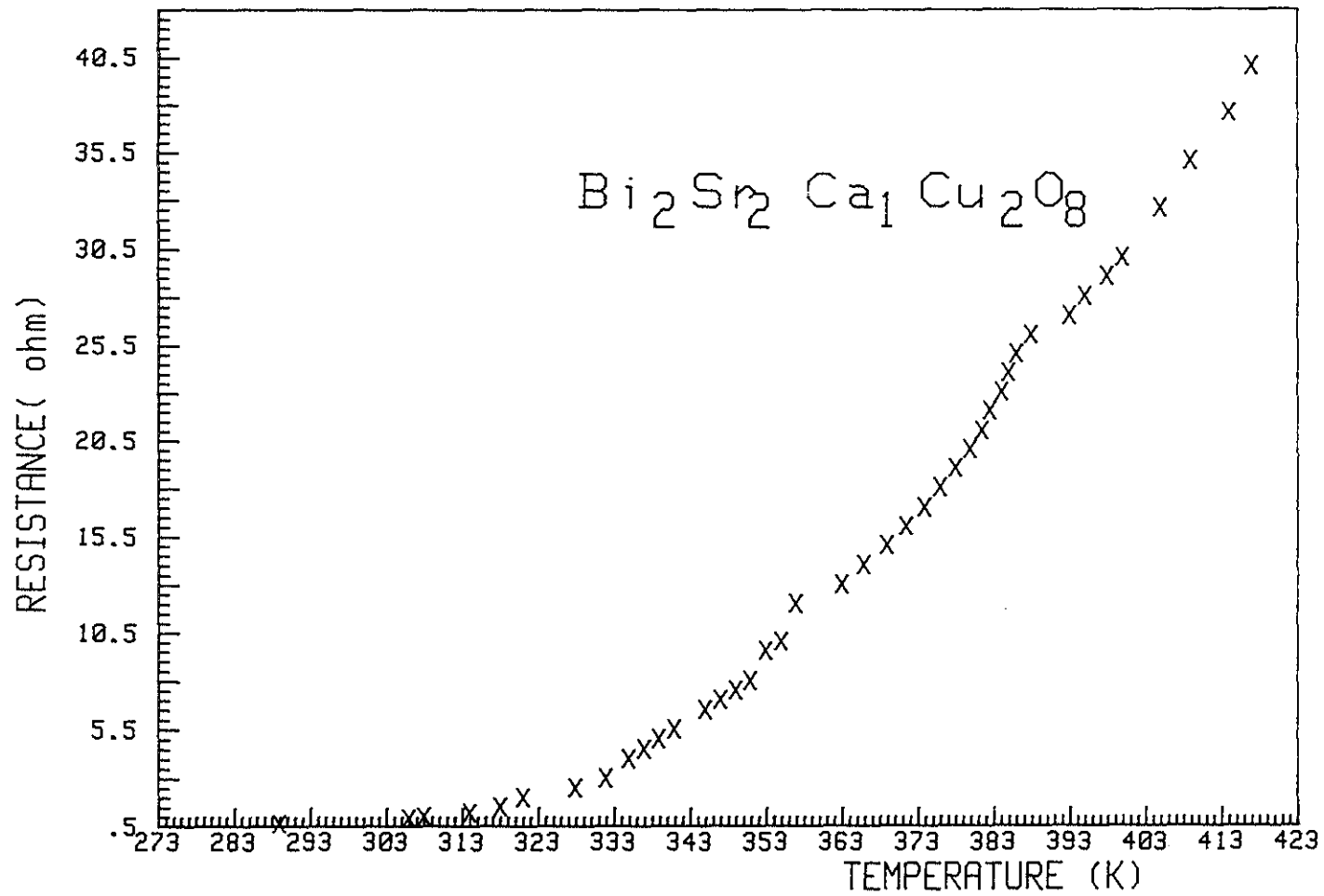


Fig.4.6 Temperature dependence of Resistance

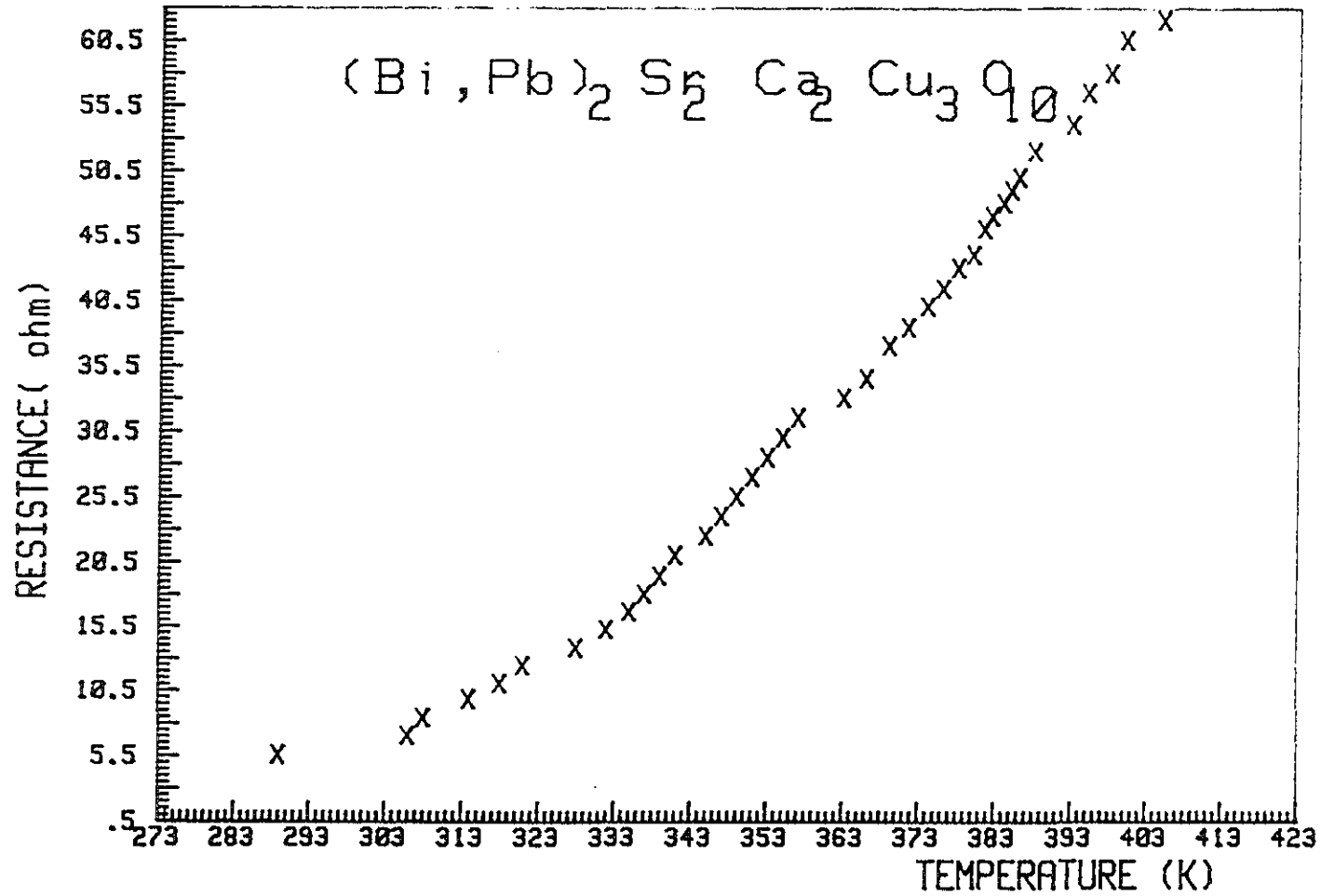


Fig. 4.7 Temperature dependence of Resistance

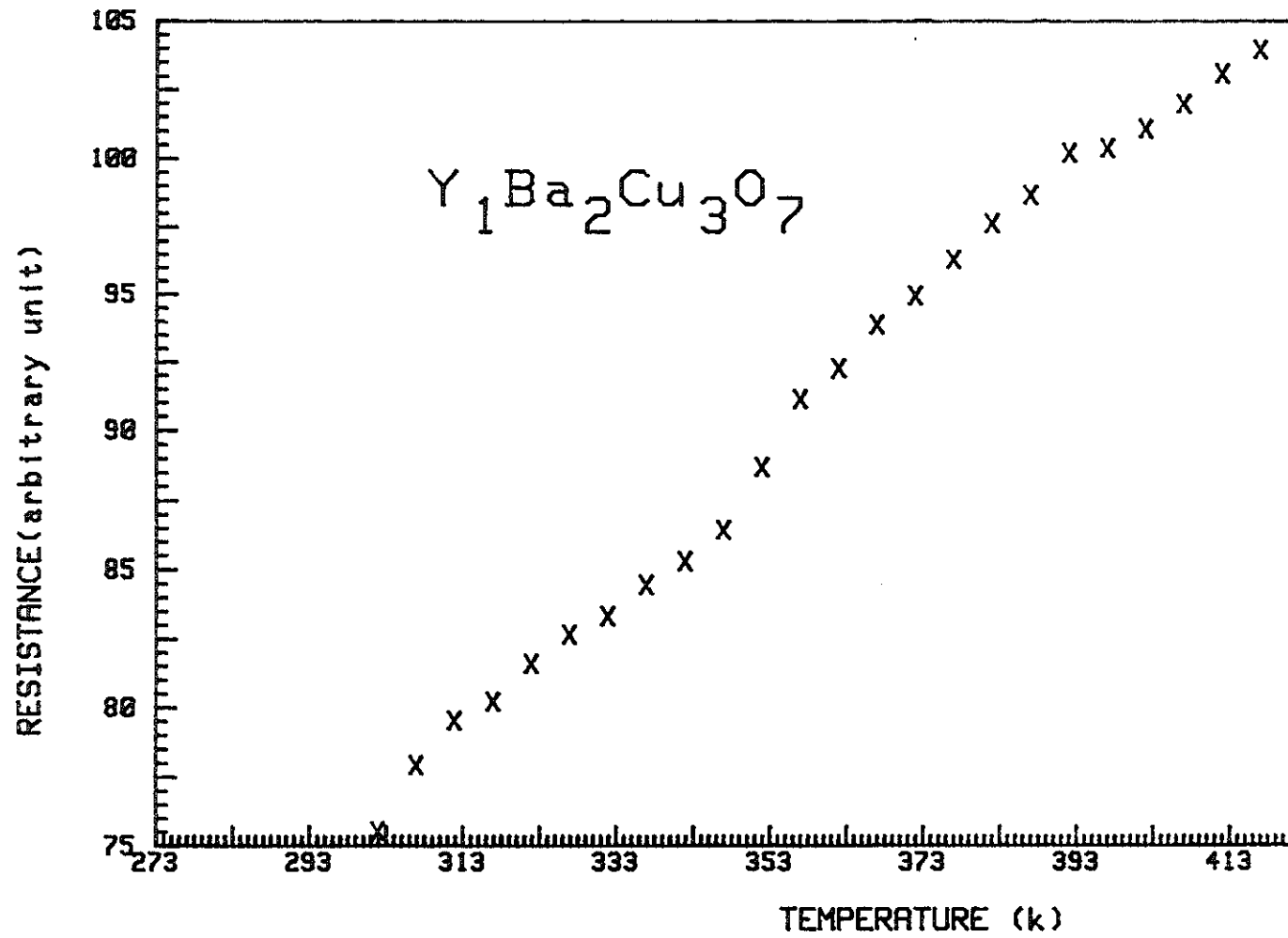


FIG. 4.8 Resistance as a function of Temperature

We use silver paste in making contacts.

Four - probe method is preferred to two - probe method since it neglects contact effect.

The electrical resistance was measured at a different temperature, starting from room temperature upwards. The results, in Fig 4.6, Fig 4.7 and Fig 4.8 indicate that the samples (high - T_c) oxide superconductors) exhibit metallic properties in this range of temperature, i.e., the resistance values showed remarkable increase with temperature. This gives a strong confirmation that the Cu-O sublattice (metallic layer) play the role in conduction process.

4.4 Hall Effect Measurement

When a magnetic field in Z - direction is applied at right angle to the direction of the electric current, an electric field is set up in a direction perpendicular to both the directions of the current and the magnetic field [33].

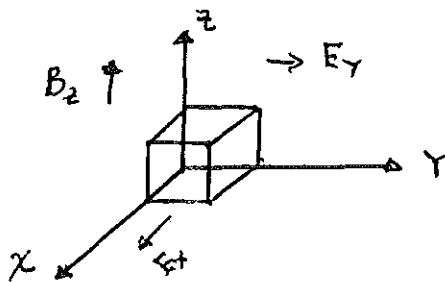


Fig 4.9 Hall effect (Directional representation)

An electric field E_y , is developed in the y direction which balances the force developed by the interaction of the electric current and the magnetic field.

The Hall voltage arises from the deflection (by applied magnetic field) of electrical charge carriers moving to the side of the conductor.

$$E_y = U_H / d$$

where U_H is the Hall voltage

d is the width of the specimen in the electric field direction

The Lorentz force on a charged particle of charge e moving with

a velocity V in a magnetic field of density B and electric field E is (in SI unit)

$$\vec{F} = e(\vec{E} + \vec{V} \times \vec{B}) \quad (4.1)$$

The Hall field developed is given by

$$\vec{E} = R_H(\vec{J} \times \vec{B})$$

where R_H is the Hall coefficient and

J is current density

$$\text{Thus, } E_y = - R_H J_x B_z \quad (4.2)$$

In a steady state, we have

$$\vec{J} = n\mu e[\vec{E} + \vec{V} \times \vec{B}]$$

where μ is the drift mobility and

n is electron density

$$\text{Thus, } J_x = n e E_x \mu \quad (4.3)$$

$$\text{and } J_y = 0 = n e E_y \mu + n e B_z \mu V_x$$

$$\text{or } 0 = n e E_y \mu + n e B_z \mu^2 E_x \quad (4.4)$$

$$\text{since } V_x = \mu E_x$$

From equation (4.3);

$$E_x = J_x / n e \mu \quad (4.5)$$

Substituting eqn. (4.5) in to eqn. (4.4)

$$E_y = - (1/ne) B_z J_x \quad (4.6)$$

From eqns.(4.2) and eqn. (4.6), the Hall coefficient is

$$R_H = - 1/ne \quad (4.7)$$

at equilibrium

$$eE_y = eB_z V_x$$

or
$$eU_H/d = eB_z V_x$$

and
$$J = nVe$$

$$I = t d n V e \quad \text{where } t \text{ is sample thickness}$$

$$\rightarrow d = I/Vnte \quad (4.8)$$

From eqns. (4.7) and (4.8)

$$R_H = U_H \cdot t / I_x B_z \quad (4.9)$$

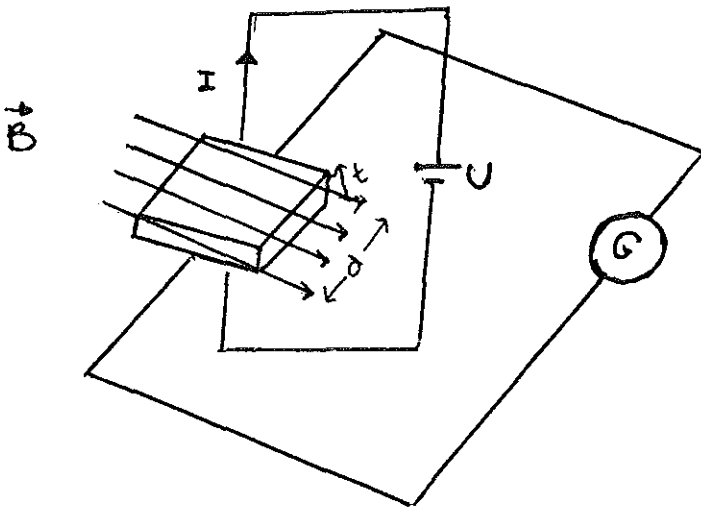


Fig.4.10 Experimental set up for Hall effect measurement

Experimental data for 123 compound

$$I_x = 1.5 \text{ A}$$

$$B_z = 4 \times 10^3 \text{ G } (0.4 \text{ A/m}^2)$$

$$t = 0.23 \text{ cm}$$

Galvanometer deflection is converted to voltage reading as

$$U_H = \theta_H \times R_g / S_1 = 0.5 \text{ mm} \times 10 \text{ ohms} / 15 \text{ mm} / \text{microA} = 0.33 \mu\text{V}$$

where $R_g = 10 \text{ ohms}$ is the galvanometer resistance

$S_I = 15 \text{ mm} / \mu\text{A}$ is the galvanometer current sensitivity

$\theta_H = 0.55 \text{ mm}$ is galvanometer deflection

$R_H = U_H \cdot t / I_x B_z = 12.6 \times 10^{-9} \text{ cm}^3$ and

$n = 1 / R_H e = 4.97 \times 10^{21} \text{ cm}^{-3}$

The published value of concentration is

$n = 8.9 \times 10^{21} \text{ cm}^{-3}$

The simple relationship between the Hall coefficient and the electronic concentration makes Hall analysis a useful experimental tool.

For 123 compound, result is with the order of the published one. But for 2223 and 2212 phase signals (Galvanometer deflection) appeared to be weak, on the level of noises. Thus Hall measurement was not reliable for the other two oxide superconductors.

4.5 Thermopower (Seebeck Effect) Measurement

Whenever the ends of two different materials are joined and maintained at different temperatures, i.e., one at temperature T and the other at $T + \Delta T$, an electromotive force (emf) is developed in

the circuit (see Fig 4.11). This emf is called the Seebeck voltage. For small temperature differences the developed emf is proportional to the temperature difference and depends on the material used to form the junction.

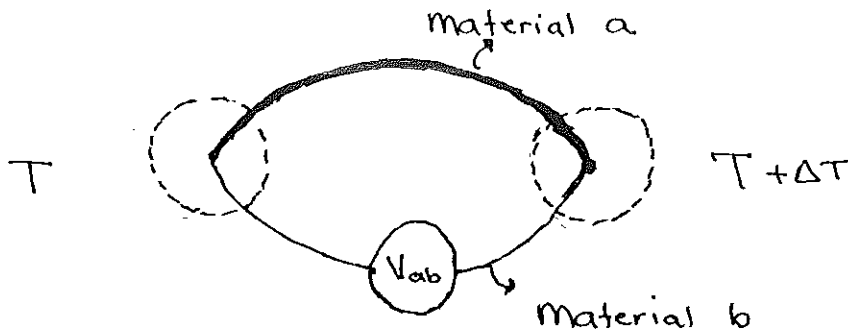


Fig. 4.11 Set - up for Thermopower

Physically, electrons near the hot junction will acquire more kinetic energy than the electrons near the cold junction. The higher - energy electrons diffuse from the hot junction toward the cold junction. This depletion of electrons at the hot end sets up an electrical potential gradient which of course, is due to the temperature gradient.

$$S = \frac{\Delta V}{\Delta T} \quad (4.10)$$

where ΔV Potential gradient

ΔT temperature gradient

S Seebeck coefficient

The experimental procedure for Thermopower measurement was as in Fig 4.12, i.e the two ends of the sample were put at different temperature T_1 and T_2 , the temperature readings were measured by thermocouple as in Fig 4.12 and the seebeck voltage due to the temperature gradient was also measured by the voltmeter.

For metals, seebeck coefficient can be given interms of Fermi energy as [32]

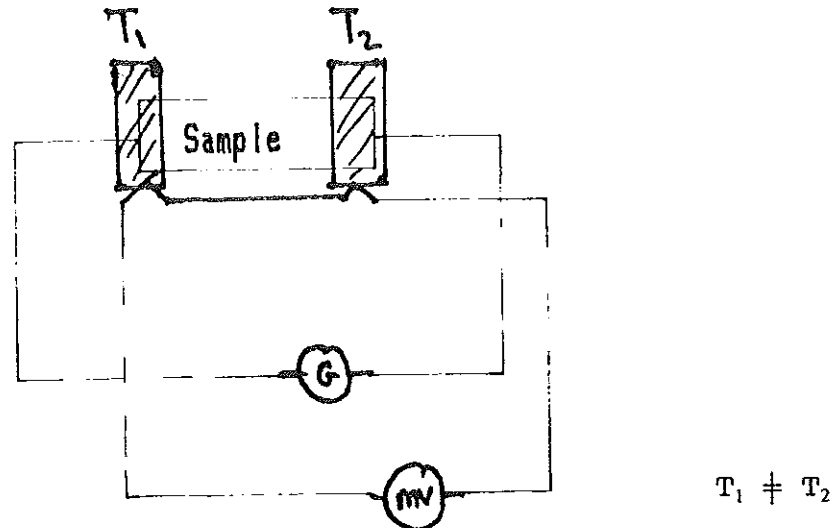


Fig. 4.12 Experimental set up for Thermopower measurements.

$$S = -\frac{k}{e} \left(\frac{\pi^2}{3} \eta^{-1} \right)$$

Where k_B is Boltzman constant

e is electric charge

η is reduced Fermi energy, $\eta = E_f/kT$

T is temperature

or

$$S = \frac{-k^2 \pi^2 T}{3eE_f} \quad (4.11)$$

Mostly, in thermopower measurement, heating is done by electrical method. But Seeback voltage is too small, Hence small induced current can affect results markedly. As in fig.(4.16) electrical heating results are affected by the induced current (noise). To avoid this problem, candle flame heating using aluminium foil which has good contact with sample is preferred. The obtained results in fig. (4.17 & 4.18) are in the same fasion as presented by others. Electrical heating is possible with more precoutions, i.e., the sample should be

screened from external electromagnetic wave effects.

From the Thermopower Vs temperature graph and using equation (4.11)

$$\text{Slope} = \frac{K^2 \pi^2}{3eE_f} \quad (4.12)$$

and Fermi energy for metals is given by

$$E_f = \frac{\hbar^2}{2m^*} [3\pi^2 n]^{2/3} \quad (4.13)$$

where h is Planck's constant by π
 n is carrier concentration density
 m^* is the effective mass of electron

In operating thermopower measurement, the magnitude of the emf generator was measured by the deflection of the galvanometer and the temperature of the sample was measured by thermocouple. The thermocouple reading was in volt, but it was calibrated so as to convert readings to units of temperature (kelvin). The calibration is in Fig 4.13.

Similar to the resistance measurement, thermopower measurements as in Fig 4.17 and Fig 4.18 showed that Oxide superconductors (samples) exhibit metallic behavior.

In addition to this, the carrier concentration was determined using the data from thermopower measurement.

In determining the carrier concentration of the oxide sample, I have plotted the thermopower as a function of temperature. The results are in Fig 4.17, Fig 4.18 and in Fig

4.19 for 2212, 123 and 2223 phases respectively. Stright line fitting of the data was made by eye observation with random error not more than 2% and the systematic error in measurement was 8% i.e the error considered was 10%.

For $Y_1Ba_2Cu_3O_7$ phase, from (Fig 4.18)

$$slope = \bar{S} = \frac{(2.49-0.84)}{(383-314)K} \times 10^{-6} V/K = 2.39 \times 10^{-8} V/K^2$$

considering 10% error, the deviation in slope will be

$$\begin{aligned} \Delta S &= \pm 0.239 \times 10^{-8} V/K^2 \\ \text{Thus } S &= \bar{S} \pm \Delta S = (2.39 \pm 0.239) \times 10^{-8} V/K^2 \end{aligned}$$

The Fermi energy for 123 phase is, from equation 4.12

$$\bar{E}_f = \frac{K^2 \pi^2}{3e} \left[\frac{1}{slope} \right] = 1.68 \times 10^{-19} J$$

and the error in fermi energy will propagate as

$$\Delta E_f = \left(\frac{\Delta S}{S} \right) \bar{E}_f = \pm 0.168 \times 10^{-19} J$$

thus

$$E_f = \bar{E}_f \pm \Delta E_f = (1.68 \pm 0.168) \times 10^{-19} J$$

and the electron density for 123 phase, from equation (4.13) is,

$$\bar{n} = \frac{1}{3\pi^2} \left[\frac{2m^* E_f}{\hbar^2} \right]^{3/2} = 8.97 \times 10^{27} m^{-3}$$

The error in electron density will propagate as

$$\Delta n = 2/3 \left[\frac{\Delta E_f}{E_f} \right] \bar{n} = \pm 0.598 \times 10^{27} m^{-3}$$

Thus for $Y_1Ba_2Cu_3O_7$

$$n = \bar{n} \pm \Delta n = (8.97 \pm 0.598) \times 10^{27} m^{-3}$$

similarly for 2212 phase from Fig 4.17

$$slope = \bar{S} = \frac{(2.37 - 1.28) \times 10^{-6} V/K}{(373 - 333)K} = 2.72 \times 10^{-8} V/K^2$$

considering 10% error, the deviation in slope will be

$$\Delta S = \pm 0.272 \times 10^{-8} V/K^2$$

Thus,

$$S = \bar{S} \pm \Delta S = (2.72 \pm 0.272) \times 10^{-8} V/K^2$$

The Fermi energy for 2212 phase is

$$\bar{E}_f = \frac{K^2 \pi^2}{3e} \left[\frac{1}{slope} \right] = 1.48 \times 10^{-19} J$$

and the error in Fermi energy will propagate as

$$\Delta E_f = \left(\frac{\Delta S}{\bar{S}} \right) \bar{E}_f = \pm 0.148 \times 10^{-19} J$$

Thus,

$$E_f = \bar{E}_f \pm \Delta E_f = (1.48 \pm 0.148) \times 10^{-19} J$$

and the electron density for 2212 phase is

$$\bar{n} = \frac{1}{3\pi^2} \left[\frac{2m^* E_f}{\hbar^2} \right]^{3/2} = 7.41 \times 10^{27} m^{-3}$$

The error in electron density will propagate as

$$\Delta n = \frac{2}{3} \left[\frac{\Delta E_f}{E_f} \right] \bar{n} = \pm 0.494 \times 10^{27} m^{-3}$$

Thus for $Bi_2Sr_2Ca_1Cu_2O_8$

$$n = \bar{n} \pm \Delta n = (7.41 \pm 0.494) \times 10^{27} m^{-3}$$

Similarly, for 2223 phase from Fig 4.19

$$\text{slope} = \bar{S} = \frac{(2.75 - 1.07) \times 10^{-6} \text{V/K}}{(392 - 309) \text{K}} = 2.025 \times 10^{-8} \text{V/K}^2$$

considering 10% error, the deviation in slope will be

$$\Delta S = \pm 0.2025 \times 10^{-8} \text{V/K}^2$$

Thus,

$$S = \bar{S} \pm \Delta S = (2.025 \pm 0.2025) \times 10^{-8} \text{V/K}^2$$

The Fermi energy for 2223 phase is

$$\bar{E}_f = \frac{K^2 \pi^2}{3e} \left[\frac{1}{\text{slope}} \right] = 1.99 \times 10^{-19} \text{J}$$

and the error in Fermi energy will propagate as

$$\Delta E_f = \left[\frac{\Delta S}{\bar{S}} \right] \bar{E}_f = \pm 0.199 \times 10^{-19} \text{J}$$

Thus,

$$E_f = \bar{E}_f \pm \Delta E_f = (1.99 \pm 0.199) \times 10^{-19} \text{J}$$

the electron density for 2223 phase is

$$\bar{n} = \frac{1}{3\pi^2} \left[\frac{2m^* E_f}{\hbar^2} \right]^{3/2} = 11.54 \times 10^{27} \text{m}^{-3}$$

and the error in electron density will propagate as

$$\Delta n = \frac{2}{3} \left[\frac{\Delta E_f}{E_f} \right] \bar{n} = \pm 0.77 \times 10^{27} \text{m}^{-3}$$

Thus for $(\text{Bi,Pb})_2 \text{Sr}_2\text{Ca}_2\text{Cu}_3\text{O}_{10}$

$$n = \bar{n} \pm \Delta n = (11.54 \pm 0.77) \times 10^{27} \text{m}^{-3}$$

4.6 Meissner Effect on High - T_c Oxides

To examine flux exclusion (Meissner effect) in high - T_c oxide superconductors, it was found that a permanent magnet in the vicinity of the sample was repelled when the sample

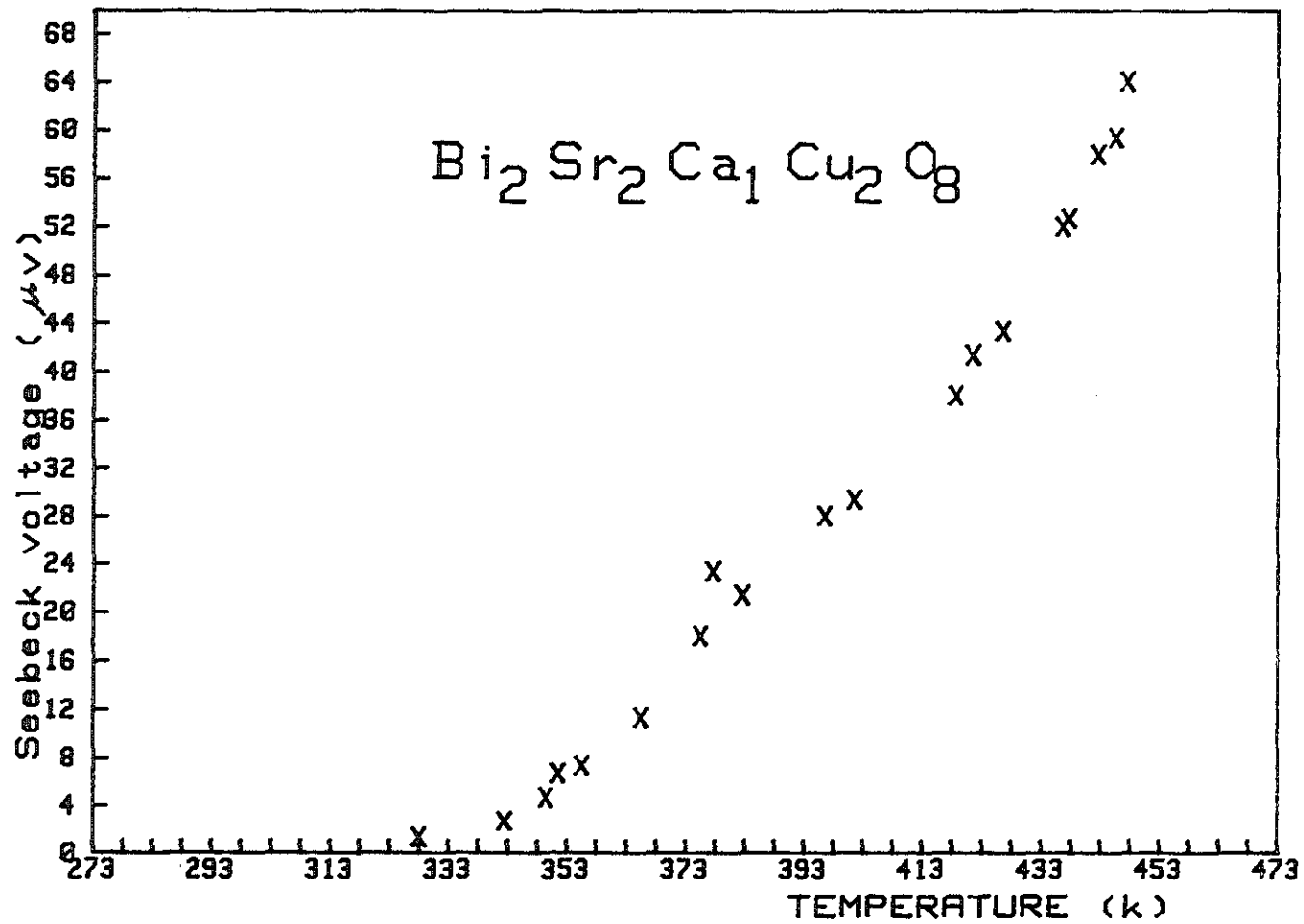


Fig. 4.14 SEEBECK VOLTAGE Vs TEMPERATURE

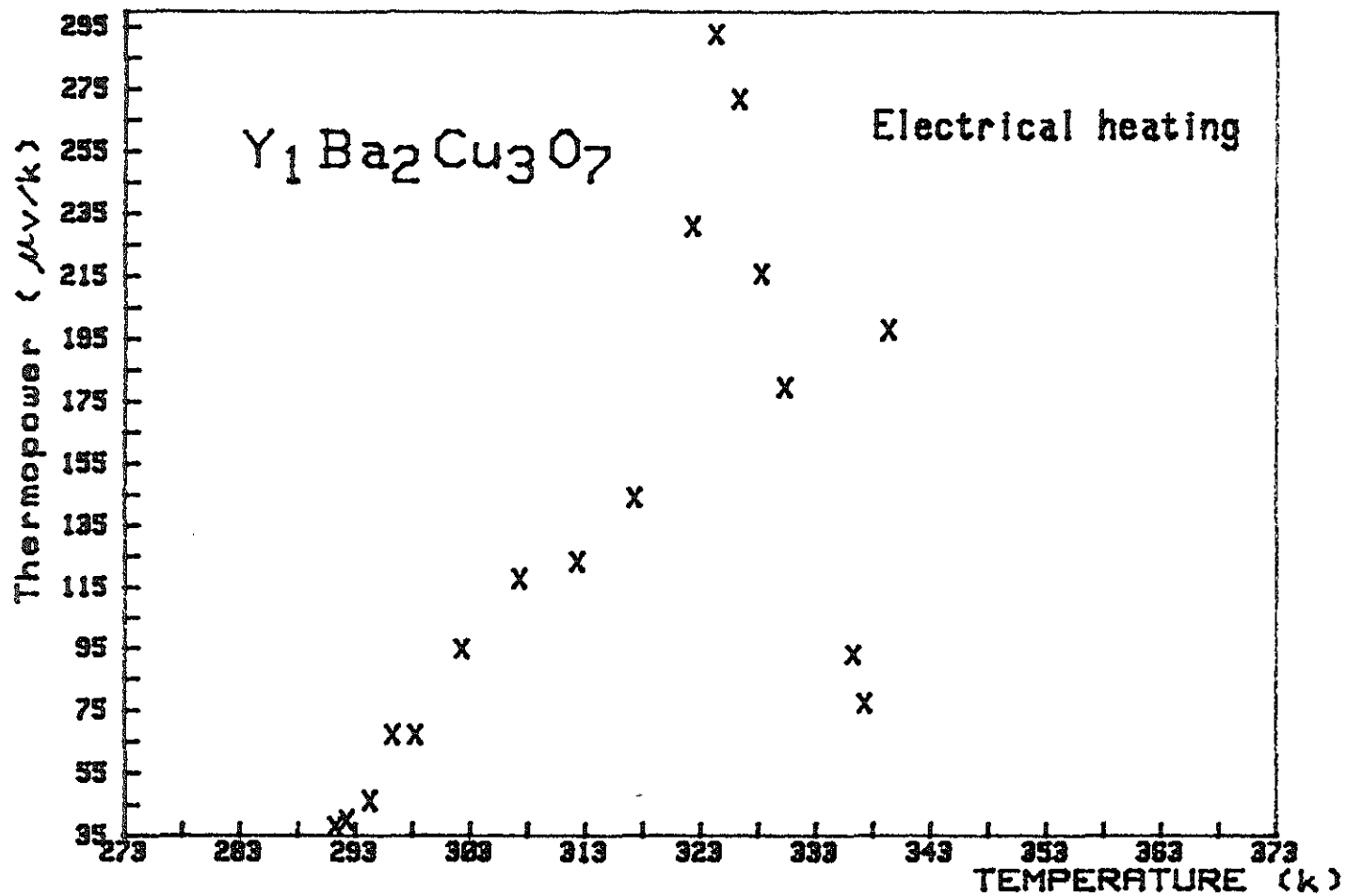


Fig. 4.15 THERMOPOWER Vs TEMPERATURE

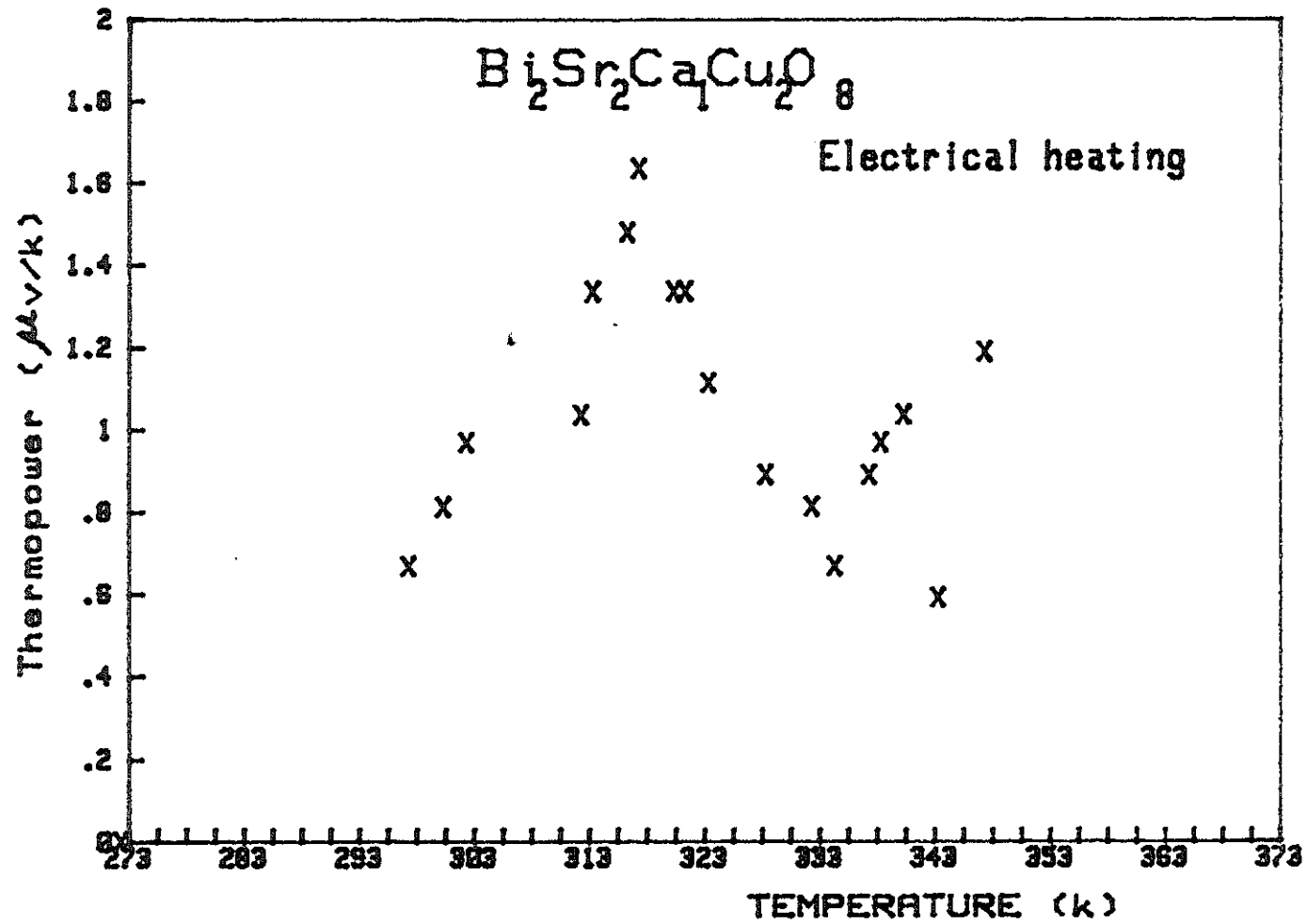


Fig. 4.16 THERMOPOWER Vs TEMPERATURE

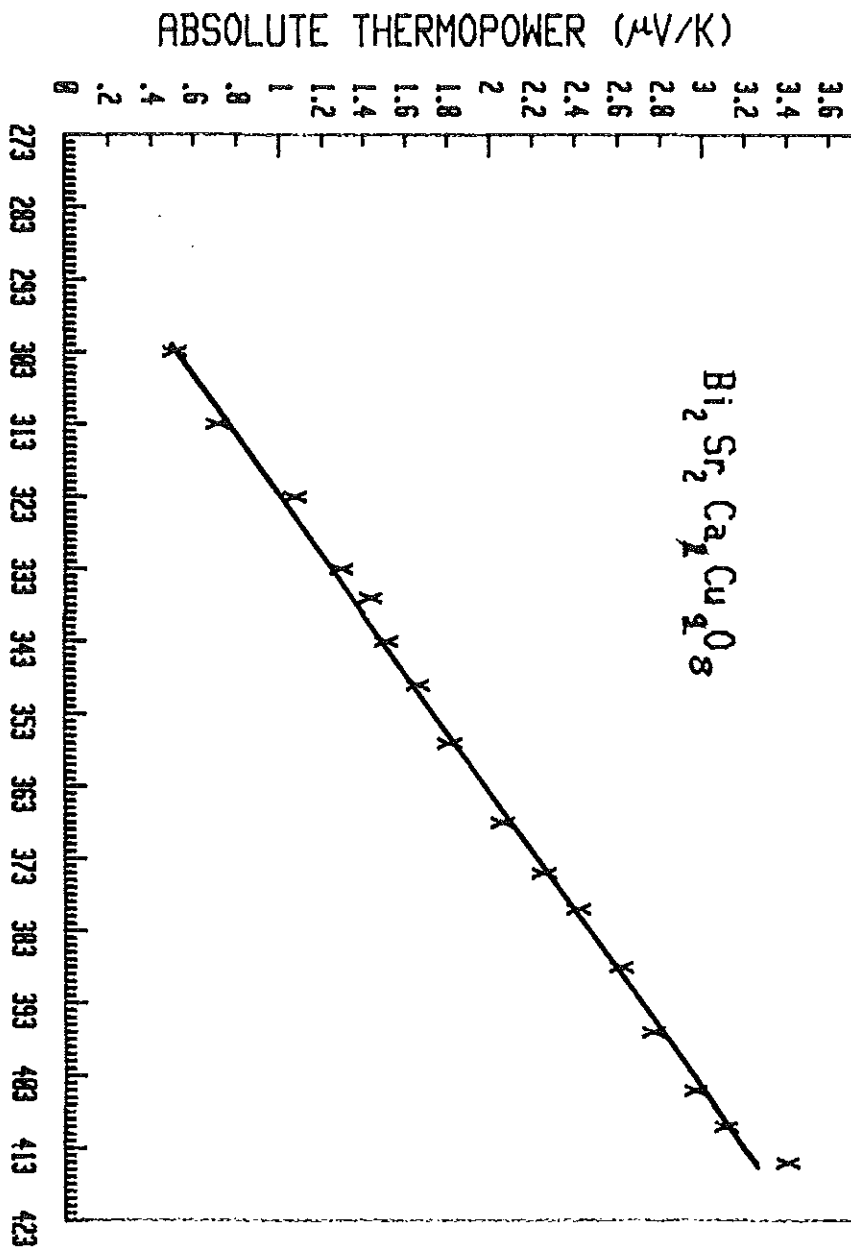


Fig. 4.17 THERMOPOWER VS TEMPERATURE

TEMPERATURE (K)

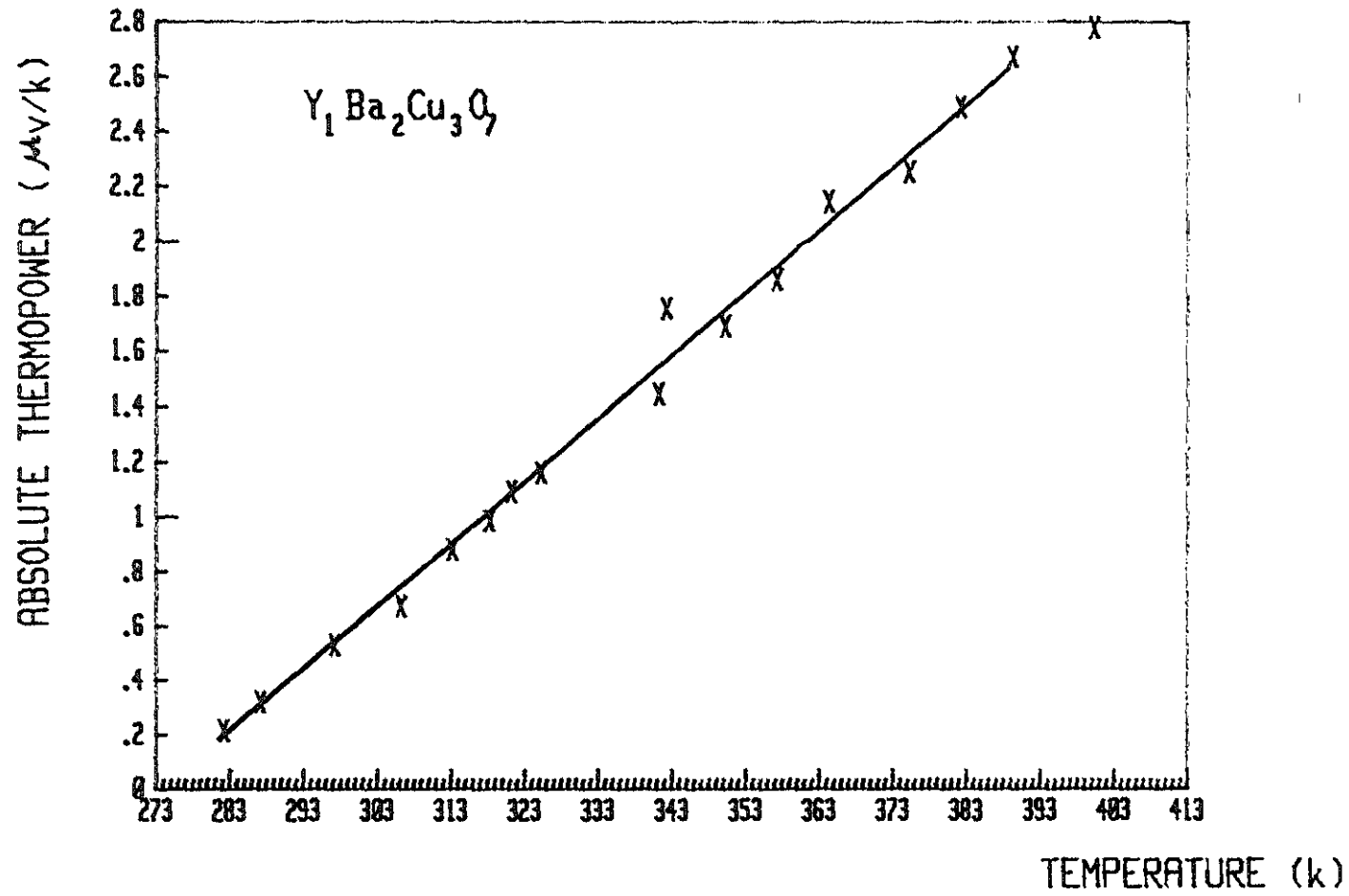
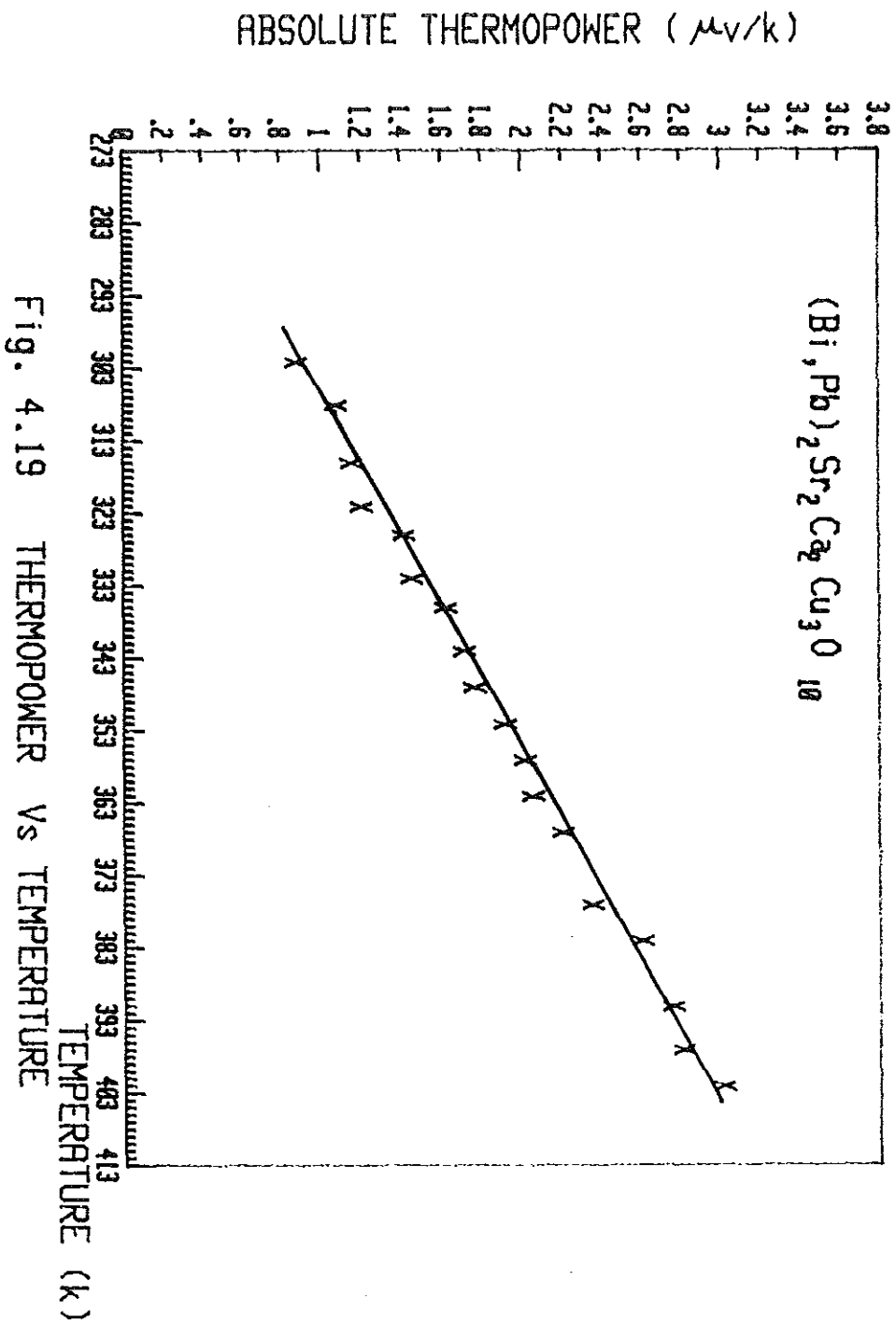


Fig. 4.18 THERMOPOWER Vs TEMPERATURE



temperature was around liquid Nitrogen temperature. The flux exclusion appeared till the temperature drops to the transition temperature, however, there is no exclusion below the transition temperature. This was an additional, evidence that our samples were superconductors. There are materials which do not exhibit Meissner effect but their resistance could drop to immeasurable quantity, and are not superconductors.

The critical current density (J_c) which is useful for practical applications for our samples are.

For 2233 phase, 8×10^5 A/cm² in c-axis and 2×10^5 A/cm² in the a-b direction at 4.2K and 0T [33].

For 123 phase, 10^7 A/cm² at 4.2K and 1T [34].

The lower critical magnetic fields (H_{c1})

For 2212, 290 ± 100 , along c-axis and 110 ± 100 , along a-b direction at 4K [35].

For 2223 phase, $330 \pm 10^\circ\text{C}$ along C - axis and $110 \pm 10^\circ\text{C}$ along a-b direction at 4K [35].

4.7 Investigation of the Transition Temperature

Using the standard Four - probe method resistance measurement (Fig. 4.20), the transition temperature (T_c) can be determined from the corresponding plots of temperature dependence of resistance given in Fig 4.21, Fig 4.22 and Fig 4.23

Each Experimental run was made by changing the temperature from liquid nitrogen temperature (77K) to room temperature, the temperature values were measured by the thermocouple set in the experiment with an accuracy of 0.5 K (caliberation of thermocouple is in Fig 4.13) and the corresponding resistance

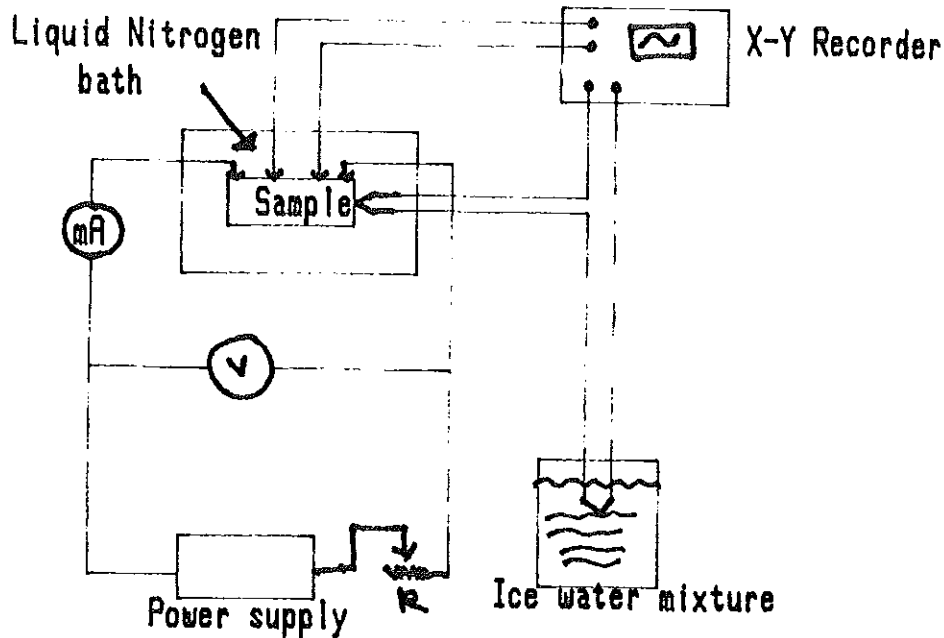


Fig. 4.20 Experiment set up for four - probe method values were measured by measuring the voltage drop across the sample allowing to pass a constant current, since for constant current voltage is proportional to resistance. The experimental setup is in Fig 4.20. The results were plotted by the x-y recorder set in the experiment, The corresponding transition temperature are

Sample	Transition temperature	Carrier concentration
$Y_1Ba_2Cu_3O_7$	90 ± 0.5 K	$(8.97 \pm 0.598) \times 10^{27} m^{-3}$
$(Bi, Pb)_2Sr_2Ca_2Cu_3O_{10}$	106 ± 0.5 K	$(11.54 \pm 0.77) \times 10^{27} m^{-3}$
$Bi_2Sr_2Ca_1Cu_2O_8$	80 ± 0.5 K	$(7.41 \pm 0.494) \times 10^{27} m^{-3}$

From ABB model, λ_{ex} (electron - exciton coupling constant) varies from 0 to 0.5 as given in equation (3.19) and the conduction mechanism of materials with critical temperature upto - 40 K is explainable. But for our oxide samples λ_{ex} related to the carrier concentration by equation (3.21), varies from 1 to 1.5 and materials with greater transition temperatures are explainable.

Using the carrier concentration determined from thermopower measurement and the transition temperatures from standard four - probe method, comparison was made by plotting the experimental data on the theoretical graph of the transition temperature (T_c) as function of log of the carrier concentration given in Fig (4.24). As in the graph, one can observe fitting of experimental data with the predicted theoretical curve. In Fig 4.24, the experimental errors in measurements are considered by putting marks which covers certain areas instead of putting points.

Thus ABB model works quite well for our Oxide samples and " exciton + phonon" mechanism could explain the conduction mechanism.

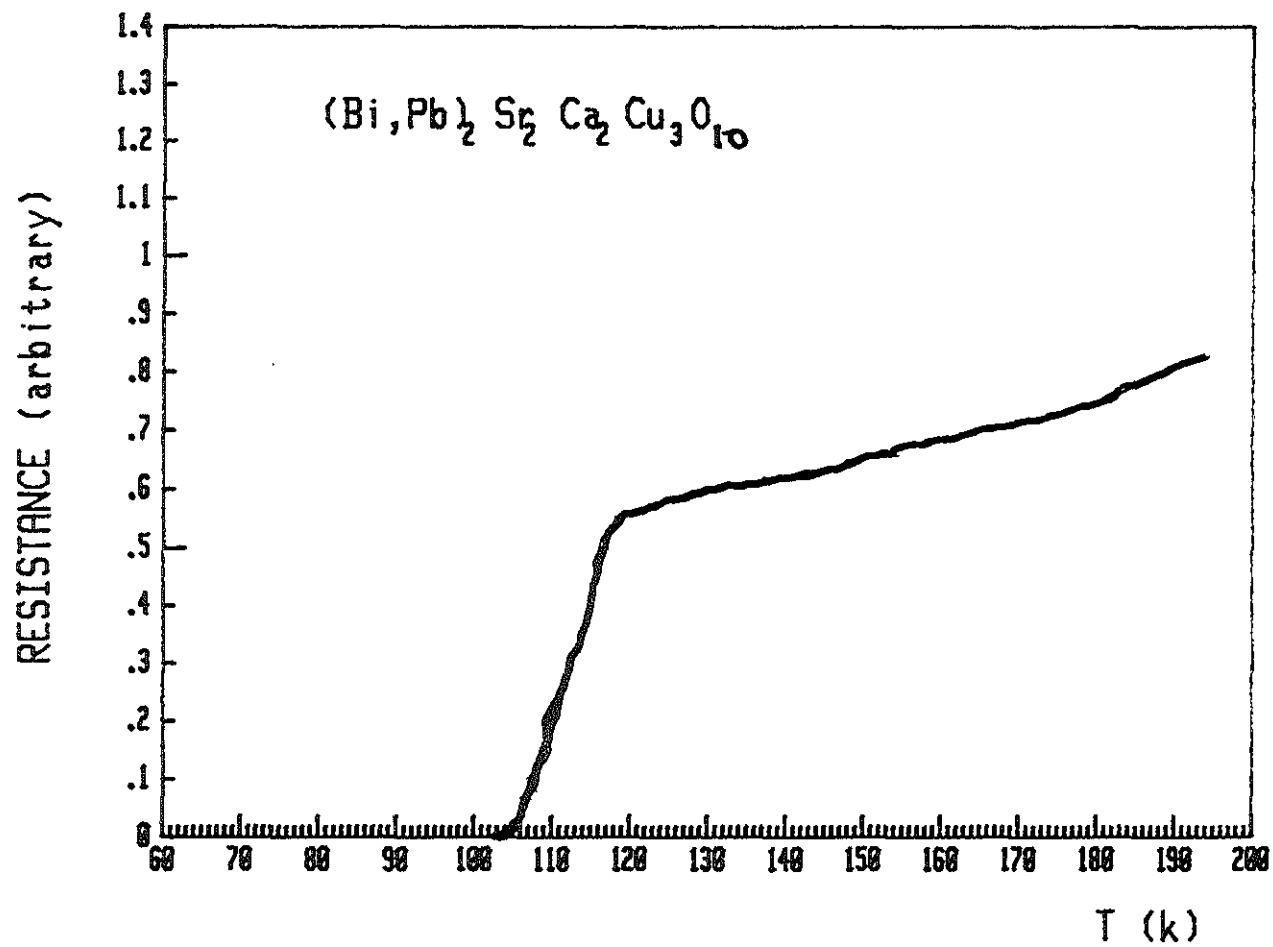


Fig. 49 Temperature dependence of the Resistance of 2223 phase

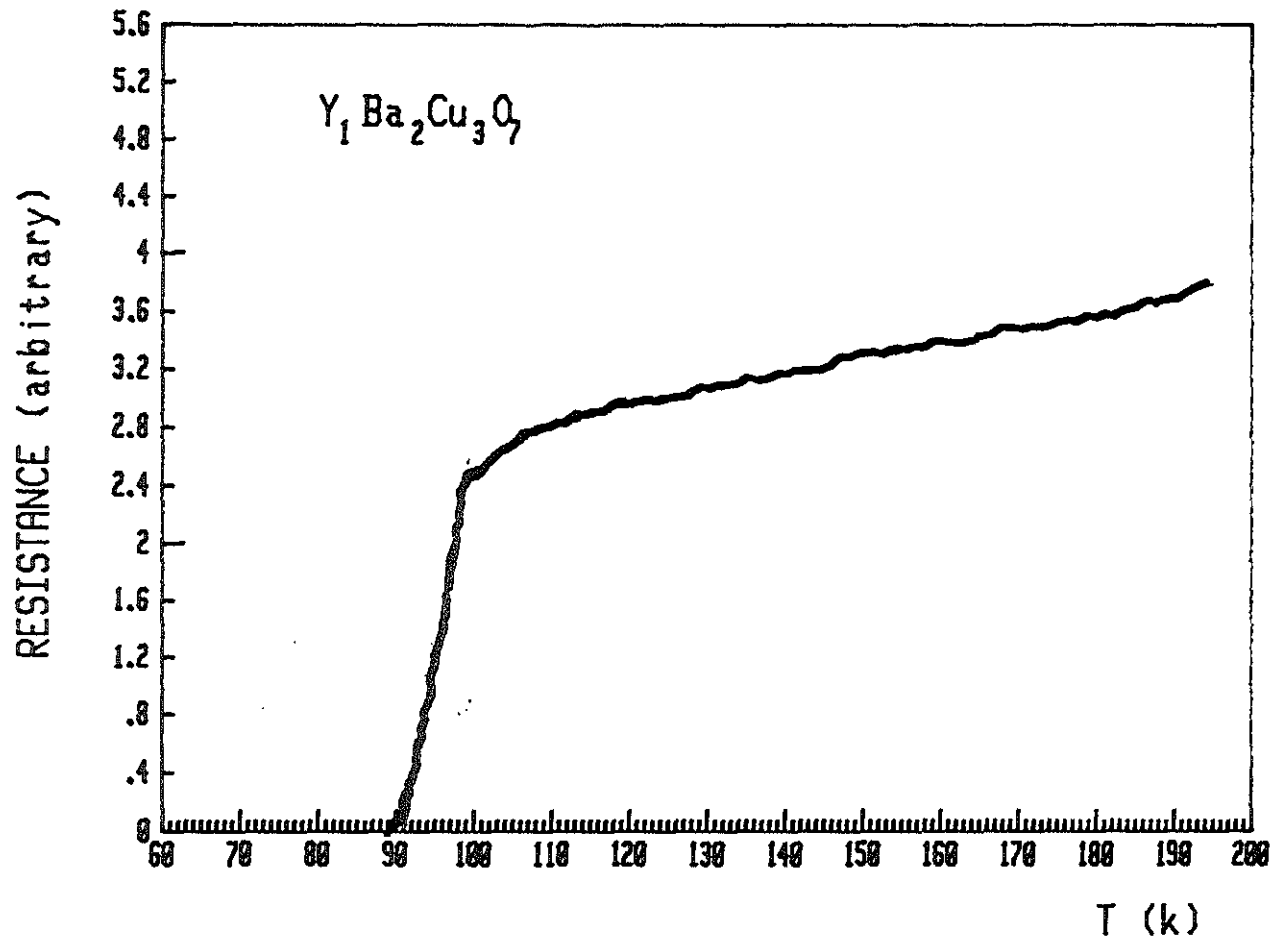


Fig. 4.22 Temperature dependence of the Resistance of 123 phase

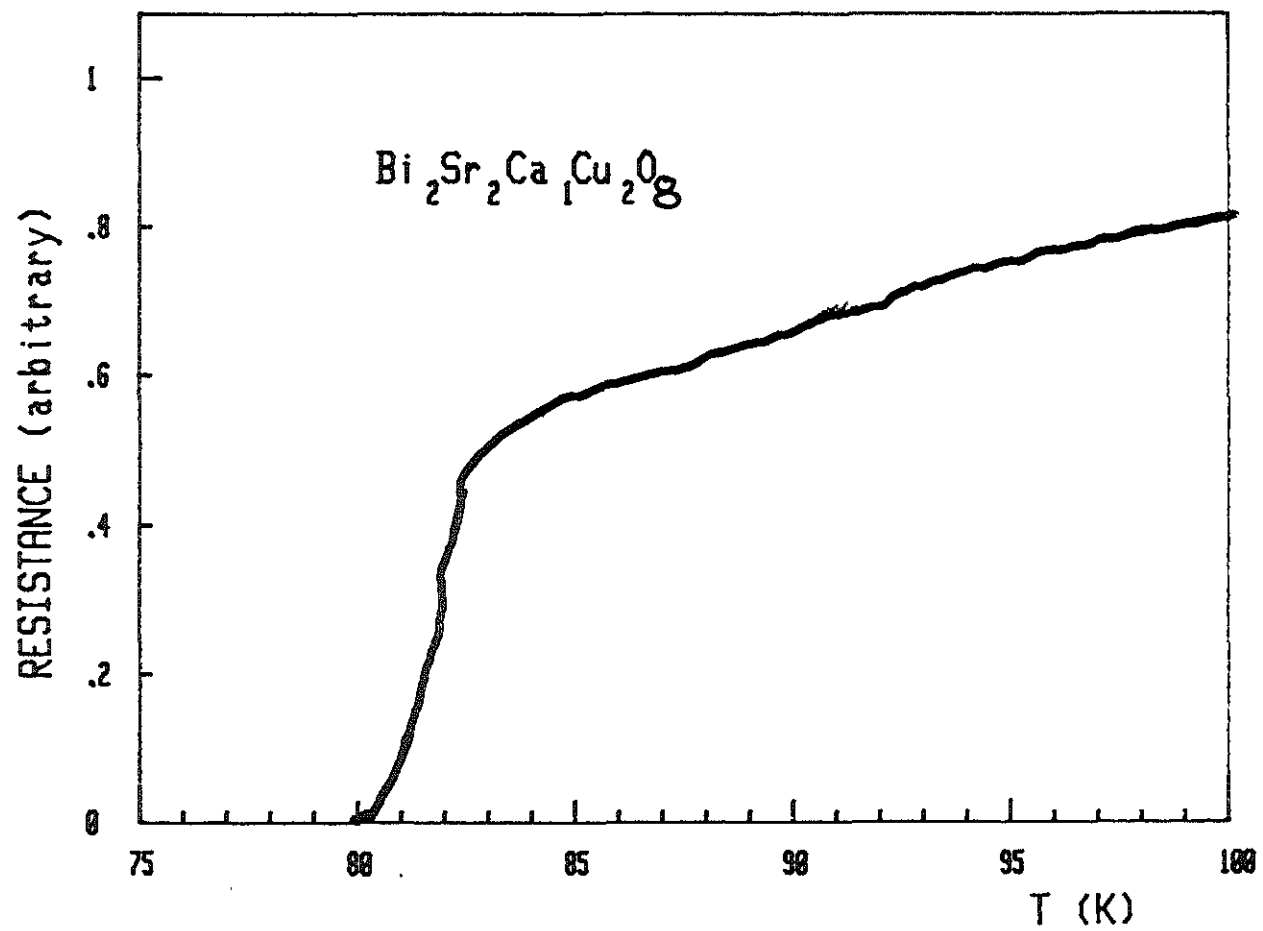


Fig. 4.23 Temperature dependence of Resistance of the 2212 phase

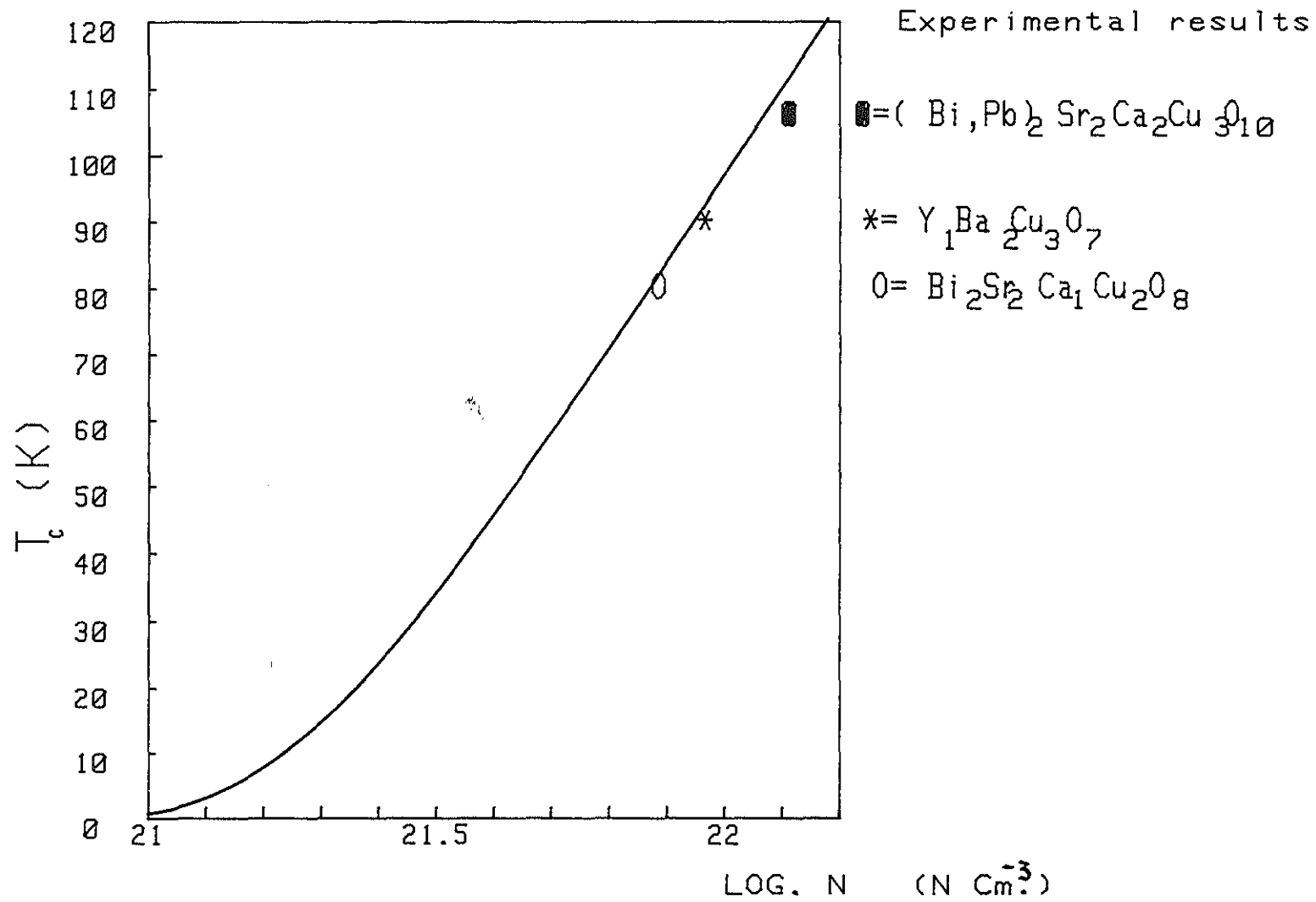


Fig. 4.24 Theoretical curve of T_c as a function of Log. carrier density

CHAPTER 5 CONCLUSIONS

1. On the basis of our experimental data investigated samples $Y_1Ba_2Cu_3O_7$, $(Bi,Pb)_2 Sr_2Ca_2Cu_3O_{10}$ and $Bi_2Sr_2Ca_1Cu_2O_8$ are ceramic high T_c superconductors with transition temperature 90 K, 106K and 80.5K respectively.
2. Structure studies reveal that we dealt with polycrystalline superconducting phases.
3. The graphs of temperature dependence of resistance and thermopower measurements indicates that our oxide samples exhibit metallic properties above their transition temperatures. This confirms that the Cu-O sublattice (metallic layer) plays the role in electrical conduction.
4. Carrier concentration were determined using thermopower effect measurement. In this measurement candle flame heating was preferred to electrical heating, since the induced current in electrical heating affects the measurement markedly. The investigated oxide samples are characterized by relative small carrier concentration when compared to metals.
5. Superconducting phase in our samples was also confirmed by observing Meissner effect.
6. Exciton mechanism is discussed with respect to ABB model :- a thin metallic layer on a semiconductor surface. This model works well for our oxide samples, since they are sandwich structure with alternating layers of metal - semiconductor metals. Based on this model " exciton + phonon " mechanism could explain superconducting mechanism

of our oxide sample. We conclude that our experimental results are sufficiently encouraging to a substantial experimental efforts to establish the exciton mechanism in the described manner with an ultimate goal of producing high temperature superconductors.

APENDIX

```

1   REM ' Program for calculating Tc as a function of carrier
    density'
10  GINIT
20  GRAPHICS ON
30  PLOTTER IS CRT,'INTERNAL'
31  PLOTTER IS 705,'HPGL'
33  PEN 3
40  VIEWPORT 20,80,20,90
50  FRAME
51  CLIP ON
60  WINDOW 21,22.2,0,120
70  AXES .1,10,21,0,.5,10
71  CLIP OFF
72  CSIZE 3,.5
79  LORG 6
80  FOR I=0 TO 120 STEP 10
90      MOVE 20.9,I+1
100     LABEL I
110 NEXT I
120 FOR I=21 TO 22.2 STEP .5
130     MOVE I,-.001
140     LABEL I
150 NEXT I
160     PEN 4
351    CLIP OFF
355 FOR I=21 TO 22.18 STEP .1
363     J=10^(I+6)
373     N=10^I
420     Lph=.015
430     M=1/3
450     Wg=.16
471     H=(1.054)/(10^34)
473     Ma=(3*9.1)/(10^31)
476     Wf1=(H*H/(2*Ma))*((3*PI*PI*J)^(2/3))
477     Wf=Wf1*(10^19)/1.6
479     M1=M/(1+M*LOG(Wf/Wg))
480     To=600
481     Wpo=To*8.62/100000
482     Lph1=Lph/(1+Lph)
483     L=((.85/(10^21))*N)^.22
484     Lex1=L/(1+L)
485     G=Lph1+((Lex1-M1)/(1-((Lex1-M1)*LOG(Wg/Wpo))))
486     T=To*.7*EXP(-1/G)
487     PRINT T,N,Wf
488     MOVE I,T
489     CSIZE .1,.01
490     LORG 2
492     LABEL '0'
493     NEXT I
494     Q=LGT(1.16*10^22)
495     MOVE Q,106
496     CSIZE 4,.4
497     LORG 2
499     LABEL ' 0  0=( Bi,Pb) Sr Ca Cu 0 '
500     MOVE 22.2,104
501     CSIZE 3,.6
503     LABEL '          2  2  2  310'
504     R=LGT(8.9*10^21)
505     MOVE R,90

```



```

1   REM 'Programme for Resistance dependence on temperature
10  GINIT
11  PLOTTER IS 705,'HPGL'
30  GRAPHICS ON
31  PEN 5
40  VIEWPORT 20,110,25,90
50  FRAME
52  WINDOW 0,150,75,105
54  AXES 1,.5,0,75,10,5,3
60  LORG 6
101 PEN 3
102 MOVE 60,100
104 LABEL 'Y Ba Cu O '
105 MOVE 63,99
106 LABEL '1 2 3 7'
108 CLIP OFF
109 PEN 3
110 DEG
120 LDIR 90
140 MOVE -14,88
141 LORG 4
143 CSIZE 3,.5
150 LABEL 'RESISTANCE(arbitrary unit)''
160 LORG 6
170 LDIR 0
180 MOVE 100,73
190 LABEL 'TEMPERATURE (k)''
191 PEN 3
240 CSIZE 2.5,.5
250 LORG 6
251 CLIP OFF
260 FOR I=0 TO 150 STEP 20
261   J=I+273
270   MOVE I,74.99
280   LABEL J
290   NEXT I
300   LORG 8
310   FOR I=75 TO 105 STEP 5
320   MOVE -.5,I
330   LABEL I
340 NEXT I
350 PEN UP
351 DIM G(2,25)
360 FOR I=1 TO 2
365   FOR L=1 TO 25
370     READ G(I,L)
371   NEXT L
372 NEXT I
373   DATA 24,30,35,40,45,50,55,60,65,70,75,80,85,90,95,100,105
      ,110,115,120,125,130,135,140,145,150
374   DATA 75.5,77.9,79.5,80.2,81.57,82.64,83.31,84.44,85.28,86
      .42,88.67,91.10,92.24,93.85,94.91,96.28
376   DATA 97.59,98.62,100.16,100.33,101.03,101.93,103.04,103.9
      ,104.51
377   PEN 4
378   FOR L=1 TO 25
379     MOVE G(1,L),G(2,L)
380     LABEL 'X'
381   NEXT L
390 MOVE 153,70
391 CSIZE 5,.4
393 LABEL 'FIG. 4.8 Resistance as a function of Temperature'
400 END

```

```

5  REM 'Program for Thermopower dependence on temperature'
10  SINIT
12  PLOTTER IS CRT,'INTERNAL'
20  PLOTTER IS 705,'HPGL'
30  GRAPHICS ON
31  PEN 5
33  VIEWPORT 20,100,20,80
34  FRAME
42  WINDOW 273,413,0,2.8
52  AXES 1,.2,273,0,10,5,3
105 CLIP OFF
106 CSIZE 4,.4
107 MOVE 293,-.6
109 LABEL 'Fig.      THERMOPOWER  Vs  TEMPERATURE'
110 DEG
120 LDIR 90
130 CLIP OFF
140 MOVE 260,.6
141 CSIZE 4,.4
150 LABEL 'ABSOLUTE THERMOPOWER (  v/k)'
170 LDIR 0
180 MOVE 393,-.4
190 LABEL 'TEMPERATURE (k)'
200 MOVE 293,2.4
210 LABEL 'Y Ba Cu O'
251 CLIP OFF
252 CSIZE 3,.3
253 MOVE 294,2.35
254 LABEL ' 1      2      3  7'
255 LORG 6
260   FOR I=273 TO 413 STEP 10
270     MOVE I,-.01
280     LABEL I
290   NEXT I
300 LORG 8
310 FOR I=0 TO 3 STEP .2
320   MOVE 273,I
330   LABEL I
340 NEXT I
351 DIM G(2,17),S(17)
360   FOR I=1 TO 2
365     FOR L=1 TO 17
370       READ G(I,L)
371     NEXT L
372   NEXT I
373 DATA 283,288,298,314,307,319,322,326,343,351,342,358,355
,375,383,390,401
374 DATA 4,6,10,16.7,12.7,18.7,20.7,22,33.3,32.0,27.3,35.3,4
0.7,42.7,47.3,50.7,52.7
375   FOR K=1 TO 17
376     S(K)=G(2,K)/19
379   NEXT K
380   FOR L=1 TO 17
381     MOVE G(1,L),S(L)
382     LABEL 'X'
383   NEXT L
400   END

```

REFERENCES

1. E.A. Lynton, Superconductivity, Methun, London, 1969.
2. G.A. Rickoyzen, Theory of superconductivity, Inter Science Publisher, New York, 1965.
3. D.N. Longenberg, Solid State Physics Source Book, McGraw Hill, USA, 1985
4. C.Kittes, Solid state physics, Johnwiley, USA, 1976.
5. D. Shoenberg, Superconductivity, Combridg University Press, London, 1960.
6. B.S. Saxena, etal, Fundamental of solid state physics, Naveen press, Merrat, 1976.
7. P.G. Degennes, Superconductivity of Metals and Alloys, Translated by P.A. Pincus, Bengamin, Newyork, 1966.
8. M. Tinkham, Introduction to superconductivity, McGrow-Hill, USA, 1975.
9. I.M. Blatt, Theory of superconductivty, Academic Press, 1964.
10. I.M. Ziman, SPrinciple of the Theory of Solids, Vikas, New Delhi, 1972.
11. W.A.Harrison, Solid state Theory, Tata McGrow-Hill, Bombay, 1970.
12. I.G. Bednorz and K.A. Muller, Z.Phys. B Condensed matter 64,189 (1986).
13. R. Beyers, etal, Appl. phy. Lett. 1987.
14. L.V. Azarof, Introduction to solids, McGrow

Hill, New York.

15. H. Mazaki, Y. Ueda, Y. Alhara, T. Kubazoe and K. Kosuge:
Ipn I. Physics 28(1989) L368.
16. E.M. Engler, R.B. Beyers, V.Y. Lee, A.Nazzal, G. Lim,
S.S.P. Parkin, P.M. Grant, J.F. Vazquez, M.L. ramirez
and R. Jacoisitz, High Temperature Superconductivity,
World scientific, Singapore, p. 25, 1985
17. R.I. Cava, A.W. Hawat, B. Batlogy, M. Marczio, K.M.
Rabe, I.I. Krajewski, W.F. Peck, L.W. Rupp, Pysics C
65,419(1990)
18. S. Ushida: Jpn. J. Appl. Physics 26, (1987) L142
19. B. Batlogy, Physics Today, USA, June 1991, p 48
20. H. Maedia, Y Tanka, M. Fukutoni, and T. Asano;Ipn. I
Appl. Physics 27(1988) L209
21. H. Nazano, R. Liany, Y. Matsunga, M. Sugiyama, M. Ttoh,
and T. Nakumura: Jnp. J. Appl. Physics 28(1989) 1364
22. H.Z. Loye, S.W. Keller, K.L. Leavy and A.M. Stacy,
Phycsics Rev. Lett 58, 2337 (1987)
23. L.C. Bourne, M.F. Crommie and A. Zett, Phycsics Rev.
Lett 58, 2337 (1987)
24. D. Alleder, I. Bray and I. Bardeen, Physics Rev. 37 1020
(1973)
25. W.L. Mcmillian, Physics Rev. 167, 331, (1968)
26. D. Pines, Elementary Excitation in Solids, Bengamin,
Newyork, 1964.
27. C.F. Gallo, L.R. Whitney and P.I. Walash, Noval

- superconductivity, Plenum Press, USA, 1987.
28. Xu Yuhuan, Li Zhangrong, Li Chaorui, Wang Hong, Li Wu and Lin Xianduan, High Temperature Superconductivity, World Scientific, Singapore, 1987, p. 87
 29. S. Kishida, H. Tokutaka, S. Nakanishi, K. Nishimori: Jpn, J. Appl. Phys., 28 (1989) L406
 30. A. Maeda, K. Noda, K. Uchinokura and S. Tanaka: Jpn. J. Appl. Phys. 28 (1989) L576
 31. T. Yougi, L. Bingxiong, Z. Wanjing, L. Zhengyi, Z. Xiangmiao and S. Meichey, High Temperature Superconductivity, World Scientific, Singapore, 1987, p. 134
 32. G.C. Jain and W.B. Berry, Transport Properties of Solids and Solid State energy conversion, Mc Grow Hill, USA,
 33. T. Umemura, A. Nazaki, K. Egawa, F. Uchikawa and K. Sato: Jpn. J. Appl. Phys. 31 (1992) 2698
 34. K. Watanabe, N. Kabyashi, S. Awaji, G. kido and Y. Muto: Jpn. J. Appl Phys. 30 (1991) L1639
 35. K. Tagya, K. Senda, T. Yosida, N. Fukuoka and H. Sasakura: Jpn. J. Appl. Phys. 31 (1992) L1170